

Thermoelectric Cooler Based Temperature Controlled Environment Chamber  
Design for Application in Optical Systems

Scott Nuo Zhang

Thesis submitted to the faculty of the  
Virginia Polytechnic Institute and State University  
In partial fulfillment of the requirements for the degree of

Masters of Science  
In  
Electrical Engineering

Anbo Wang, Chair  
Gary Pickrell  
Yizheng Zhu

May 6, 2013  
Blacksburg, Virginia

Keywords: Thermoelectric Cooler, PID Control, Thermal Management

Copyright 2013, Scott N. Zhang

# Thermoelectric Cooler Based Temperature Controlled Environment Chamber Design for Application in Optical Systems

Scott N. Zhang

## **Abstract**

Temperature control is widely sought after in regards to optical systems as their optical parameters often show dependence on temperature. Examples include diode lasers, multiplexing systems, optical amplifiers, and filters all of whom have a high sensitivity to temperature. This thesis presents a temperature controlled environment chamber actuated by a thermoelectric cooler. The design of which provides a simple, multi-applicable solution for temperature control in optical devices.

The final device is comprised of three sub-areas of design. Each subsystem was custom built and applied in the final assembly – including a digitally implemented signal generator, an error correction controller, and the environment chamber heat sink structure. The signal generator is used as input for a switched-mode based Peltier driver found commercially. A feedback error controller compensates the driver for temperature control. Both systems are implemented with microcontroller units. The environment chamber heat sink assembly is designed specifically to handle the thermal energy generated by the thermoelectric cooler.

All of the systems were tested collectively for functionality. The input signal generator achieved its design goals and is capable of creating specific profiles in the temperature response. Error controller performance was reasonable in set-point tracking for continuous input signals. Step input responses are tuned for minimal settling time and overshoot. Temperature resolution in the thermistor response is around  $0.1^{\circ}\text{C}$  after digital filtering. The thermal design achieved its goal of operating in an ambient environment up to  $54^{\circ}\text{C}$ . Low temperature ambient environment operation has been confirmed to  $8^{\circ}\text{C}$ .

## **Acknowledgements**

I would first like to express my gratitude and appreciation to my advisor Dr. Anbo Wang. I am indebted for this opportunity and grateful for my acceptance under his tutelage. I am thankful for his guidance and support, and feel fortunate for having had this chance to study and collaborate with such an excellent research group. I would also like to thank the other members of my committee for their service and assistance.

I would like to thank my project manager Dr. Bo Dong for the insight and extensive experience he has shared with me. I would also like to thank my first project manager Dr. Dorothy Wang for her guidance and patience during my first few months with the lab.

In addition, I would like to thank all present and former members of CPT that I have had the privilege to work with and learn from. Special thanks to Michael Fraser, Tyler Shillig, Di Hu, Li Yu, and Amiya Behera for their help, encouragement, and friendship over these past two years.

Finally, I would like to give thanks to my family. My parents have always been endless sources of inspiration, support, and guidance. My siblings have been important role models for my life.

# Table of Contents

|   |     |
|---|-----|
| Acknowledgements.....                                   | iii |
| Table of Contents.....                                  | iv  |
| List of Figures.....                                    | vi  |
| Nomenclature.....                                       | vii |
| Chapter 1 Introduction.....                             | 1   |
| 1.1 Project Motivations.....                            | 1   |
| 1.1.1 Design Requirements.....                          | 2   |
| 1.2 Thesis Overview.....                                | 2   |
| Chapter 2 Literature Review.....                        | 4   |
| 2.1 Thermoelectric Coolers.....                         | 4   |
| 2.2 PID Control.....                                    | 6   |
| 2.2.1 Implementation Issues.....                        | 7   |
| 2.3 Chamber Heat Sink and Thermal Dissipation.....      | 10  |
| Chapter 3 Electrical Design and Implementation.....     | 14  |
| 3.1 Electrical System Requirements.....                 | 14  |
| 3.2 Component Selection.....                            | 16  |
| 3.2.1 PIC Microcontroller Units.....                    | 16  |
| 3.2.2 Peltier Current Drivers.....                      | 17  |
| 3.2.3 TEC Modules.....                                  | 18  |
| 3.3 Circuit Design.....                                 | 19  |
| Chapter 4 Control System Design and Implementation..... | 21  |
| 4.1 Error Correction Implementation.....                | 21  |
| 4.2 Temperature Profile Generation.....                 | 22  |
| 4.3 External Synchronization.....                       | 25  |

|  |    |
|--|----|
| Chapter 5 Environment Chamber Design Assembly .....        | 27 |
| 5.1 Thermoelectric Heat Rejection .....                    | 27 |
| 5.1.1 Parameter Extraction.....                            | 27 |
| 5.1.2 Waste Heat Formulation .....                         | 28 |
| 5.2 Heat Sink Optimization.....                            | 29 |
| 5.3 TEC Housing Chamber.....                               | 31 |
| 5.3.1 Component Swapping.....                              | 31 |
| 5.3.2 Thermally Conducting Walls.....                      | 32 |
| 5.3.3 Thermal Compound .....                               | 33 |
| Chapter 6 Experimental Analysis of System Performance..... | 34 |
| 6.1 Experimental Setup.....                                | 34 |
| 6.2 Step Response Tuning.....                              | 35 |
| 6.3 Set-point Tracking Response .....                      | 36 |
| 6.3.1 Fixed-point Tracking .....                           | 37 |
| 6.3.2 Waveform Tracking.....                               | 38 |
| 6.4 Ambient Temperature Response.....                      | 40 |
| 6.5 System Noise .....                                     | 41 |
| Chapter 7 Conclusion and Future Work .....                 | 43 |
| 7.1 Summary of Work.....                                   | 43 |
| 7.2 Suggestions for Future Work.....                       | 45 |
| References.....  | 47 |
| Appendix A – Example PID Implementation.....               | 48 |
| Appendix B – Heat Sink Thermal Design Calculator.....      | 52 |
| Appendix C – Electrical Schematics.....                    | 54 |

# List of Figures

|   |    |
|---|----|
| Figure 2.1. Typical Peltier module depiction and image of the TEC used [2] [3].....                               | 5  |
| Figure 2.2. Typical temperature feedback control system block diagram.....  | 6  |
| Figure 2.3. Basic PID controller representation.....  | 7  |
| Figure 2.4. Heat flow by conduction through a uniform slab.....   | 11 |
| Figure 3.1. Gain response of two TEC modules with different maximum cooling capacities. ....                      | 19 |
| Figure 3.2. Custom fabricated TEC controller circuit. ....  | 20 |
| Figure 4.1. Thermistor voltage model for temperature waveform generator. ....                                     | 23 |
| Figure 4.2. Oscilloscope reading of external synchronization in action.....                                       | 25 |
| Figure 5.1. Modeled cooling capacity performances for TEC 06311-5L31-05CFL.....                                   | 28 |
| Figure 5.2. Generated waste heat for different TEC temperature gradients.....                                     | 28 |
| Figure 5.3. Total heat transfer for different heat sink dimensions and fluid flow rates.....                      | 30 |
| Figure 5.4. Final heat sink and fan assembly.....   | 31 |
| Figure 5.5. Rendering of environment chamber design.....  | 32 |
| Figure 5.6. Two surfaces without thermal compound (a), and with thermal compound (b). ....                        | 33 |
| Figure 6.1. Block diagram of experimental setup.....  | 34 |
| Figure 6.2. Raw signal response to step input signal. Close up of rising and falling edge.....                    | 35 |
| Figure 6.3. Percent error response of data in Figure 6.2.....   | 36 |
| Figure 6.4. Fixed set-point input with raw and filtered response. ....  | 37 |
| Figure 6.5. Percent error response of the fixed-point tracking experiment. ....                                   | 38 |
| Figure 6.6. Raw and filtered response signals for sinusoidal and triangle wave input.....                         | 39 |
| Figure 6.7. Filtered temperature response of system with ambient temperatures of approximately 54°C and 8°C. .... | 40 |
| Figure 6.8. Differential EMI measured at 1cm from an inductor on the controller circuit board.                    | 41 |
| Figure 6.9. Variation in reference voltage during a fixed set-point operation.....                                | 42 |

# Nomenclature

Thermoelectric cooler variables and symbols:

|          |   |
|----------|---|
| $Q_c$    | Cooling capacity, absorbed thermal energy           |
| $Q_h$    | Dissipated heat, rejected heat, total heat transfer |
| $I$      | Thermoelectric cooler current                       |
| $n$      | Number of thermocouple elements                     |
| $\alpha$ | Thermocouple Seebeck coefficient                    |
| $R_e$    | Internal electrical resistance of couple element    |
| $K_e$    | Thermal conductance of couple element               |
| $W_o$    | TEC input electrical power                          |
| $T_h$    | TEC hot side temperature                            |
| $T_c$    | TEC cold side temperature                           |

PID controller variables and symbols:

|                |                                  |
|----------------|----------------------------------|
| $k_p$          | Proportional control gain        |
| $k_I$          | Integral control gain            |
| $k_D$          | Derivative control gain          |
| $u_c(t)$       | Time domain control signal       |
| $e(t)$         | Time domain error signal         |
| $r(t)$         | Time domain reference signal     |
| $y(t)$         | Time domain process signal       |
| $n(t)$         | Time domain noise signal         |
| $U_c(s)$       | Laplace domain control signal    |
| $U_c^{nf}(s)$  | Laplace domain noise free signal |
| $U_{noise}(s)$ | Laplace domain noise signal      |
| $R(s)$         | Laplace domain reference signal  |
| $Y(s)$         | Laplace domain process signal    |
| $N(s)$         | Laplace domain noise signal      |
| $\tau_f$       | Derivative filter time constant  |

Thermal design variables and symbols:

|             |  |
|-------------|--|
| $Q$         | Heat transfer (general)                        |
| $k$         | Slab thermal conductivity                      |
| $A$         | Surface area of heat transfer                  |
| $T_1$       | Slab temperature reference one                 |
| $T_2$       | Slab temperature reference two                 |
| $L$         | Slab thickness                                 |
| $h$         | Heat transfer coefficient                      |
| $T_s$       | Sink temperature                               |
| $T_{fl}$    | Ambient fluid temperature                      |
| $k_{fl}$    | Fluid thermal conductivity at film temperature |
| $L_c$       | Characteristic length                          |
| $Re$        | Reynolds number                                |
| $Pr$        | Prandtl number of fluid at film temperature    |
| $\rho_{fl}$ | Fluid density                                  |
| $V_{fl}$    | Fluid flow velocity                            |
| $\mu_{fl}$  | Fluid dynamic viscosity                        |
| $\nu_{fl}$  | Fluid kinematic viscosity at film temperature  |
| $Q_{tot}$   | Total heat transfer                            |
| $A_f$       | Single fin surface area                        |
| $A_{tot}$   | Total fin surface area                         |
| $\eta_f$    | Single fin efficiency                          |
| $\eta_o$    | Overall fin efficiency                         |
| $\beta$     | Fin efficiency sub-function                    |
| $n_f$       | Number of fins                                 |
| $b_f$       | Fin height                                     |
| $t_f$       | Fin thickness                                  |
| $Z_f$       | Fin spacing                                    |
| $L_s$       | Heat sink length                               |
| $W_s$       | Heat sink width                                |



# **Chapter 1**

## **Introduction**

This thesis presents the design of a temperature controlled environment chamber, with the intention of providing a versatile, controlled, small form factor environment for optical systems. The chamber will be used to maintain constant temperatures in variable ambient temperatures as well as generating waveform specific temperature profiles within a closed environment. This can be useful in applications of laser wavelength modulation by temperature tuning or placing optical devices at fixed temperatures for reference or maintaining operable conditions in harsh ambient environments [1].

Several systems use the thermoelectric effect to control and maintain temperatures in various devices. Most notably in optics are probably distributed feedback (DFB) lasers which often contain a thermoelectric cooler (TEC) within its packaging to tune the laser's temperature. However, several other optical devices also respond to temperature dependence, and achieving the same high quality temperature control is desired. Aside from DFB lasers and other optical transmitters, operating temperature is important for optical amplifiers, multiplexers and sensors [1]. A standardized means of control is lacking for these devices, and this project hopes to provide a solution. This thesis presents the design, research, fabrication, and testing of a TEC based temperature controlled environment for application with several optical devices.

### **1.1 Project Motivations**

The primary motivation for this work is to provide the lab with a repeatable temperature control system without having to find suitable commercial products for every application. The set of design algorithms formulated over the course of this project are of particular value as they should help guide the design of future systems with modified requirements. Applications of specific interest for the fabricated device include maintaining fixed temperatures amid a range of ambient temperatures and generating flexible temperature profiles. The practical implementation of a controlled environment chamber is useful, and can help provide an added degree of assurance in temperature sensitive systems.

### ***1.1.1 Design Requirements***

In addition to the motivations addressed above several design objectives are expected in the system's performance or operation. These include:

- ***Limited commercialized product involvement.*** Complete thermoelectric temperature controllers are commercially available, as well as compact computer modules for processing and control. However utilizing these products would defeat the versatility of the system. The objective is to design a low cost system that may be created and applied in several applications.
- ***Long term temperature stability.*** The product is intended to be capable of operating continuously for several hours or even longer. If the system begins to drift or becomes unstable after time it cannot be used. A proper error correction system is necessary to maintain control and accuracy.
- ***Synchronized waveform generation.*** When a temperature profile output is desired, it sometimes becomes necessary for the temperature control system to operate synchronously with the companion system. This allows the companion system to match signal events to precise temperatures in a reliable manner.
- ***Automated and manual set-point operation.*** The system should allow operation in two modes. In automated mode, user required interaction should be limited, and the control system should be capable of continuous operation. When in manual mode, the user should freely be able to modify the system.

## **1.2 Thesis Overview**

This thesis is organized into seven chapters with introductory material found in the first two chapters. The next three chapters contain the system design and methodology for specific subsections of the device. The last two chapters contain experimental results, discussion, and closing matter.

Motivations and objectives of the research effort were outlined in Chapter 1. Chapter 2 provides a literature review of the device's subsystems. The chapter discusses the current understanding of TEC operation, PID control, and thermal management design. Chapter 3 details the electrical

design process highlighting electrical specifications, device components, and circuit design. Chapter 4 covers the software development of the system. The chapter gives an overview of the waveform generation program and PID control algorithm. Chapter 5 outlines the analysis used to design the device's environment chamber and heat sink assembly. Chapter 6 presents the results following the experimental procedure and a discussion of performance issues. Finally, Chapter 7 concludes with a summary of work and provides suggestions on improving the system design.

## **Chapter 2**

### **Literature Review**

Designing a temperature controlled environment chamber requires considerations of many sub-systems. In particular, such a device requires a mechanism to modify and alter the chamber temperature as desired. In order to control the mechanism in a meaningful manner an accurate and well-tuned controller is necessary. After the establishment of the controller, a proper vehicle to maintain and house the environment must be implemented. This chapter briefly discusses the major component in each of the subsystems that were used in the design and fabrication of the final device.

#### **2.1 Thermoelectric Coolers**

While several temperature control mechanisms exist, the focus of this particular thesis is on thermoelectric devices. In thermoelectric materials, thermal energy can be converted into electrical energy as in a thermoelectric generator (TEG) or vice versa. For the purpose of this project, using electrical energy to create a specific temperature response is the main objective. These devices, which convert electrical energy to thermal are known as thermoelectric coolers. Coolers are made up of several individual elements known as thermocouples which consist of two dissimilar materials. When an electromotive force (EMF) is applied across the two materials, heating or cooling occurs depending on the applied direction. Jean Peltier is attributed with discovering this effect in 1821, and is why TECs are often referred to as Peltier modules [2].

More commonly today, thermocouple elements are made of a junction between a p-type and an n-type semiconductor. When a number of these thermocouples are linked electrically in series and thermally in parallel a TEC module like the one seen in Figure 2.1 is formed. There are several attributes to thermoelectric devices that make them promising candidates for this project. Thermocouple elements can be manufactured with small form factors, giving the device several potential shapes and sizes. Additionally, as a solid-state device, TECs have no moving parts. In contrast to mechanical refrigerant systems, this provides the device with much longer operation lifetimes. Finally, modules used with properly tuned control systems experience more stable

steady state temperatures than their more common commercial counterpart, vapor-compression systems. These systems often experience a temperature fluctuation when configured for a fixed set-point [3].

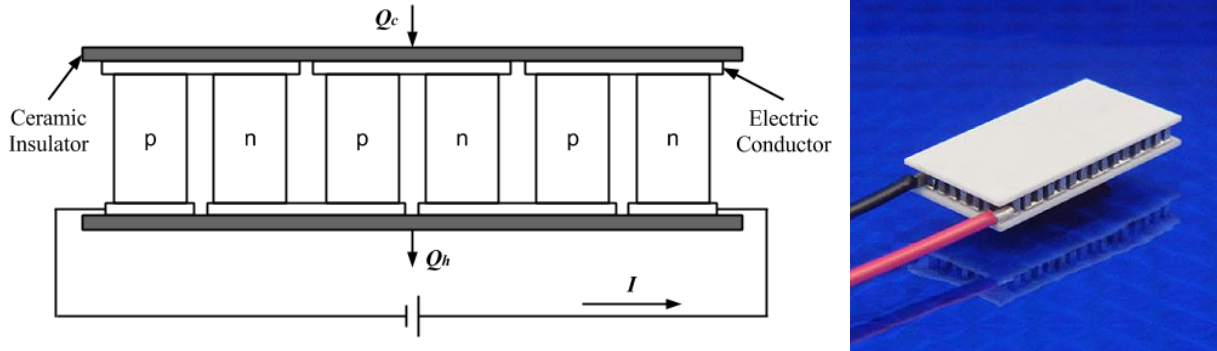


Figure 2.1. Typical Peltier module depiction and image of the TEC used [2] [3].

When thermal energy is actively transported across a medium it is called a heat pump. The TEC absorbs a quantity of thermal energy and transfers it from one side of the device to the other. In Figure 2.1 the top cold side absorbs  $Q_c$  watts of thermal energy where it contributes as a portion of the total thermal energy  $Q_h$  released from the module. The energy absorbed, or the cooling capacity of the TEC, is always smaller than the radiated energy which also includes the work performed by the EMF through Joule heating. The cooling capacity is a function of the junction temperature, the current applied, and a thermocouple material property known as its *Seebeck coefficient*. Governing equations related to  $Q_c$  and  $Q_h$  are defined below:

$$Q_c = n \left[ \alpha T_c I - \frac{1}{2} I^2 R_e - K_e (T_h - T_c) \right] \quad \text{eq. 2.1}$$

$$W_o = n [\alpha I (T_h - T_c) + I^2 R_e] \quad \text{eq. 2.2}$$

$$Q_h = Q_c + W_o \quad \text{eq. 2.3}$$

The analysis made in selecting an appropriate device for the system is found in Chapter 3 as restrictions for the selection are primarily based on electrical requirements. The equations above, however, are cardinal in the thermal management analysis of the system and are used in detail in Chapter 5. For a brief detailing of thermal constraints see Section 2.3.

## 2.2 PID Control

The error correction algorithm adopted for the system is a proportional, integral, and derivative (PID) controller. PID systems are three-term control systems and are used ubiquitously in industry [4] [5] [6]. Figure 2.2 illustrates the block diagram of the basic temperature feedback control system. The PID controller serves as a component of the control block, where each term generates a different control action. In the actual system, the *Plant* is the TEC, the *Sensor* is a thermistor, and a microcontroller unit comprises the other half of the control block.

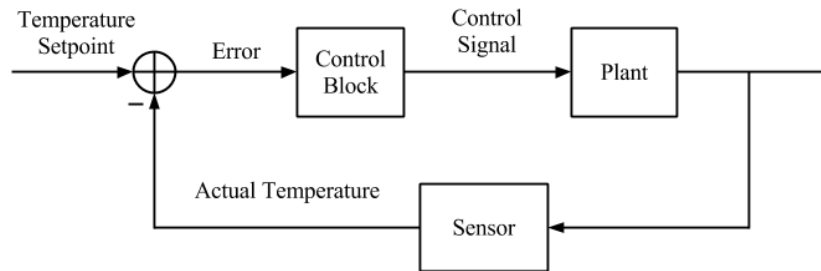


**Figure 2.2. Typical temperature feedback control system block diagram.**

The control block can be individually represented in the same manner depicted in Figure 2.3. Proportional control generates a control action that is proportional to the error signal, the difference between the set-point and the actual signal. An integral control of the error compensates for any steady offset from the set-point. Integral control in conjunction with proportional control overcomes the need for excessively large proportional gain when trying to remove steady state offset error. Derivative control utilizes the change in error over time to help compensate the signal. Derivative control is useful in damping the ringing response for a shorter settling time in the output response. Care, however, is advised in using derivative control as it can easily amplify input noise into unstable responses [4] [5] [6]. The equivalent time domain representation of the actions described above is shown in eq. 2.4, below [4]:

$$u_c(t) = k_p e(t) + k_i \int e(\tau) d\tau + k_D \frac{de}{dt} \quad \text{eq. 2.4}$$

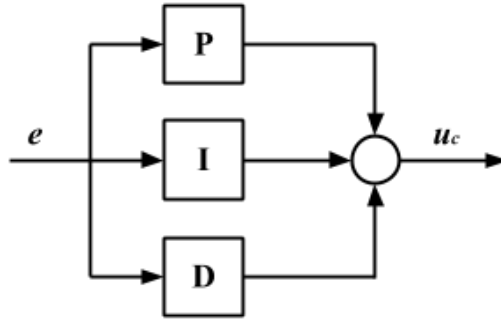


Figure 2.3. Basic PID controller representation.

Tuning of the PID controller can be performed by understanding the effects each term has on the response. Table 2.1 illustrates the behavior of each term as related to the tuning specification. Following these guidelines the present system has been tuned to shorten settling time when reaching a steady state signal, while also trying to minimize system overshoot. These two effects are inversely correlated as typically when trying to compensate for one effect, the other is exacerbated [4] [7].

Table 2.1. Tuning effects of PID controller terms [4] [5] [8].

|          | <i>Transient Response</i>   | <i>Steady State Response</i>  | <i>Tuning Comments</i>   |
|----------|---|---|--|
| <b>P</b> | Increasing $k_p$ generates faster response  | Increasing $k_p$ reduces steady state offset but does not remove it | Increasing $k_p$ increases control signal bandwidth; expect greater signal oscillation with faster control response  |
| <b>I</b> | Increasing $k_i$ generates several responses depending on transient signal, may be unstable           | Introducing $k_i$ eliminates steady state offset over time          | Increase integration time when fixed input and stable output are required; expect response time to be slower   |
| <b>D</b> | Increasing $k_d$ generates several responses and may be unstable, but can be tuned to dampen response | Introducing $k_d$ has no effect on steady state behavior            | Consider transience of input signal; low frequency input can afford longer derivative time for greater dampening; expect oscillations for higher frequencies |

### 2.2.1 Implementation Issues

When implementing PID control there are several common problems that can occur in the system response. The problems that present themselves as potential issues in the TEC controller

are addressed here as well as a discussion on each problem's solution. These issues are feedback noise gain, proportional kick, derivative, kick, and integral windup. Briefly explaining each issue; feedback noise refers to noise on the thermistor voltage signal that the control block reads as the actual temperature. This noise can have a dramatic effect on the derivative control term, and as previously mentioned requires careful attention when tuning the derivative term [5]. Proportional and derivative kick both refer to a spike in the control signal that results from a step response in the reference signal [4]. The kick response will often result in overshoot of the output response, which is not acceptable for the TEC controller application. The last issue, integral windup, arises from the limitations on the TEC current by the controller chip. Windup occurs when the integral term sums errors for durations when the TEC current is in saturation or at the current limit. Summing errors while the actuator, in this case the Peltier driver, is saturated will delay the effective control action until the integrator is unwound [5].

Feedback noise can be understood in greater detail by recognizing the construction of the PID operation. It is evident that there is a derivative amplification based purely on noise when the true error signal approximation is made. Every system has noise and thermistor sensors are no exclusion. In deriving a solution the time domain error signal can be approximated as:

$$e(t) = r(t) - y(t) - n(t) \quad \text{eq. 2.5}$$

In the Laplace domain, if the control operation is applied to the error signal approximation, it can be seen that the operation is comprised of a noise free control term and a purely noise dependent term [4] [5]:

$$U_c(s) = U_c^{nf}(s) - U_{noise}(s) \quad \text{eq. 2.6}$$

$$U_c^{nf}(s) = \left[ k_P + \frac{k_I}{s} + k_D s \right] (R(s) - Y(s)) \quad \text{eq. 2.7}$$

$$U_{noise}(s) = \left[ k_P + \frac{k_I}{s} + k_D s \right] (N(s)) \quad \text{eq. 2.8}$$

Looking at the noise dependent control term, it is clear that the derivative term responds with increasing signal amplification for increasing noise frequency. The solution to this response is to



apply a low-pass filter on the derivative term. This can be done by incorporating a pole into the derivative term. Effectively, the noise amplification is reduced by compensating the gain for higher frequencies. The Laplace domain solution for feedback noise gain can be represented in the following form [4]:

$$U_c(s) = \left[ k_P + \frac{k_I}{s} + \frac{k_D s}{\tau_f s + 1} \right] (R(s) - Y(s) - N(s)) \quad \text{eq. 2.9}$$

In proportional and derivative kick, the cause is simple. A large change in the error signal, results in an immediate response by the proportional term,  $k_P E(s)$ . Additionally, differentiating over the error signal for a step response would subsequently create an impulse like response in the control signal. Both issues create a potential overshoot effect in the output. However, the remedy is as simple as the cause. By operating the proportional and derivative terms on the process output signal instead of the error signal the effects of rapid reference signal changes are attenuated [4]. The overall response of the output signal may be slower, but the control signal is less aggressive and safer for the system as a whole. A time domain expression of the adjusted structure, often referred to as I-PD control, is seen below [4] [6]:

$$u_c(t) = -k_P y(t) + k_I \int^t e(\tau) d\tau - k_D \frac{d}{dt} y(t) \quad \text{eq. 2.10}$$

When tuning this remedy careful consideration in regards to balancing acceptable overshoot against overall system response is necessary. The application mode of the controller should also be factorized as other solutions may be more appropriate for set-point tracking or load disturbance rejection [6].

Integral windup is a definite issue with the TEC controller system. In a non-ideal system, the set-point signal would request from the PID control that the TEC current continuously increase or decrease with the magnitude of the set-point signal. However, realistically the driver has a current limit which acts as a saturation point in the real control signal. The unreal or PID control action may be responding to a larger current application from the set-point signal, but the driver

will be unable to respond. The saturation of the control signal means the closed-loop system becomes open and unstable [4] [5] [6]. For the system this means the module is operating at the driver current limit and is continuously cooling or heating the sensing surface, based on the polarity of the current. Under saturation windup occurs since the integral term is continuously compounding the response error, but the process signal is responding to a different real control signal. The residual summations delay future response as the integral action requires more time to integrate out the previously calculated false errors.

The solution to preventing integral windup is to create a digital response on the integral term. As soon as the control signal reaches the saturation region, the integration action should be turned off [4] [5] [6]. Implementing this by software would consist of applying a conditional statement that would check if the output control signal exceeded the saturation limit and setting the integral gain to zero until the control signal is no longer in saturation. This approach should reduce overshoot caused by extended periods of the control action remaining in the saturation region [4].

A discussion of the actual control implementation found in the system is addressed in Chapter 4. Performance of the PID controller can be viewed in Chapter 6 where a look at the system's response to a step input is made. Appendix A also provides an example implementation of a pure PID control program scripted on the platform of the microcontrollers used in the test system. The example institutes a general PID control algorithm with only the three term control actions implemented.

### **2.3 Chamber Heat Sink and Thermal Dissipation**

An often neglected element regarding TEC systems concerns the thermal management of the device. In any system that generates heat a means to disperse that heat is necessary. In industry, heat sinks are the most common practice in dissipating thermal energy, and the literature regarding heat sink design is quite extensive. However, most often this literature regards only the management for electrical systems [9]. The models and analysis concerning thermoelectric devices are comparatively lacking [10]. Reasons for a more structured analysis are largely due to

the notable temperature dependence in TEC performance. The specific analysis used in creating the system's housing will be described in greater detail in Chapter 5, while here a discussion on the basic principles governing heat sink design is served.

Heat sinks follow two basic modes of heat transfer: conduction and convection. Conduction involves the diffusion of heat through a solid or stationary fluid. When the transfer occurs to a fluid in motion, the mode is referred to as convection [11]. For a heat sink, both transfer modes are used in the analysis to describe the heat removal from the source to the ambient environment. In its most basic form, conduction can be defined by eq. 2.11. The heat transfer is seen to be a function of the medium's thermal conductivity, dimensions, and the temperature gradient across [11]. A conceptual illustration of the heat flow is modeled in Figure 2.4.

$$Q = kA \frac{T_1 - T_2}{L} \quad \text{eq. 2.11}$$

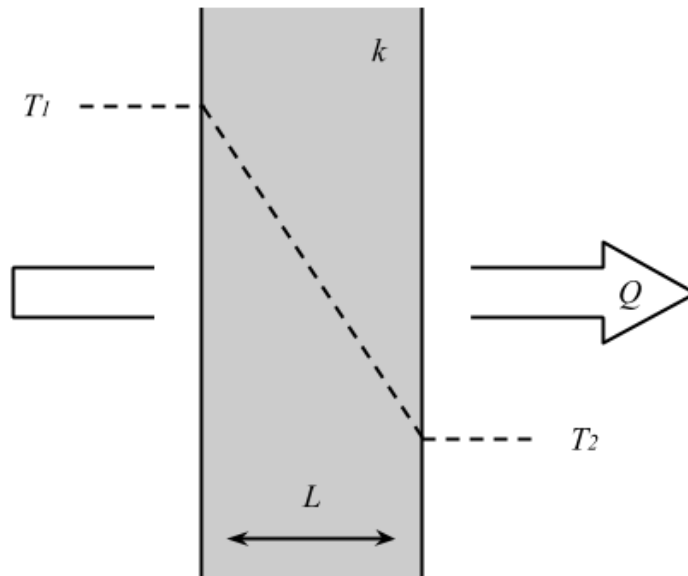


**Figure 2.4. Heat flow by conduction through a uniform slab.**

Upon reaching the ends of the heat sink or the sink-to-air interface, the convection in the ambient environment must be considered. Convection may be natural or result from a forced source. In natural or free convection, motion results from a temperature gradient in the fluid itself [2] [11].

The simplest understanding comes from knowing that hot air rises, while cool air falls and a cycle of rotating air can occur. Under forced convection, fluid is actively passed over the sink surface. In a generalized form, convective heat transport follows an equation relating the heat transfer coefficient,  $h$ , to the surface-to-fluid temperature difference, and the exposed surface area (eq. 2.12). However, with dependence on the sink geometry, the material system, and convection method used, optimizing the thermal design is actually quite involved. A walk-through and several empirically derived approximations are listed below. These equations were directly used in the thermal analysis documented in Chapter 5.

$$Q = hA(T_s - T_{fl}) \quad \text{eq. 2.12}$$

For a forced convection system, the heat transfer coefficient can be expressed by:

$$h = \frac{k_{fl}}{L_c} 0.664 Re^{\frac{1}{2}} Pr^{\frac{1}{3}} \quad \text{eq. 2.13}$$

Where:

$$Re = \frac{\rho_{fl} V_{fl} L_c}{\mu_{fl}} = \frac{V_{fl} L_c}{\nu_{fl}} \quad \text{eq. 2.14}$$

From eq. 2.12, it can be seen that heat flow is directly proportional to surface area. To increase surface area, most often, heat sinks are created with protrusions for greater heat dissipation. The protrusions have a functional efficiency,  $\eta$ , dependent on the number of protrusions and their geometry. For planar fin protrusions like the ones used in the system, the generalized heat transfer equation can be expressed as [2]:

$$Q_{tot} = \eta_o A_{tot} h (T_s - T_{fl}) \quad \text{eq. 2.15}$$

Where:

$$\eta_o = 1 - n_f \frac{A_f}{A_{tot}} (1 - \eta_f) \quad \text{eq. 2.16}$$

$$\eta_f = \frac{\tanh(\beta)}{\beta} \quad \text{eq. 2.17}$$

$$\beta = b_f \left( \frac{2h}{k_s t_f} \right)^{\frac{1}{2}} \quad \text{eq. 2.18}$$

$$A_{tot} = n_f(A_f + L_s Z_f) \quad \text{eq. 2.19}$$

$$A_f = 2(L_s + t_f)b_f \quad \text{eq. 2.20}$$

$$n_f = \frac{W_s}{(Z_f + t_f)} \quad \text{eq. 2.21}$$

With these equations it is possible to derive optimized heat sink geometries from a given fluid flow velocity, or vice versa. In this project, the latter is computed from available heat sink options. Complete realization of the thermal design is provided in Chapter 5.

## Chapter 3

# Electrical Design and Implementation

In order to keep the system unique everything from the TEC driver to circuit protection must be designed manually. The electrical system should address issues such as how the TEC module will be driven, what mechanism should be used for signal input, and how to compensate if a subsystem should fail? This chapter discusses the methodology and considerations behind the electrical system design.

### 3.1 Electrical System Requirements

The first step in the electrical design is to recognize the system's desired limitations. With the questions above in mind several specifications are formulated to simplify and reduce options. In particular, the electrical system design has the following requirements:

- ***Single supply operation.*** System power should derive from a single source. This requirement simplifies the design, limits external connections, and restricts options on system components. If necessary, other supply voltages can easily be generated by regulator circuits. The designed operating voltage is 5V.
- ***Switched mode based current driving.*** TEC controllers can be operated by two driving modes: linear or switched. Linear mode systems are comparatively simpler to design, however, they suffer from greater power inefficiencies [1]. This usually translates into a requirement for heat sink designs for the linear controller. Switched mode drivers have much greater efficiencies, but may suffer limitations regarding filter components and electromagnetic interference generation [1]. Switched mode based TEC control is selected to minimize system dimensions and make circuit level heat sink requirements unnecessary.
- ***Bidirectional TEC current supply up to 3A.*** TEC modules come in a variety of sizes, shapes, and operable conditions. As a general rule, increasing driving current allows for greater cooling capacities (eq. 2.1). However, the material composition and geometry of the thermocouple elements have definite electrical properties and a current limit. Equally, the elements' thermal properties define limits on the operable

temperature range of the device. Increasing cooling capacity of the system will allow greater bandwidth of tuning speeds; however, a sacrifice to the gain or temperature response will occur. When selecting a TEC for use, these two relationships should be considered. Presently, designing the system for a 3A current supply should permit an acceptable operating temperature range while maintaining a timely tuning response for general application.

- ***Digital PID control implementation.*** A digital controller option allows for increased customization of the correction algorithm. Finely tuning an analog PID circuit can be cumbersome and is limited by the components selected [12]. Adjustment on an analog system would require excessive effort and an appropriate understanding of analog circuit design. With a digital implementation, tuning can be more intuitive and adjustments are made by reprogramming. Issues associated with passive elements such as drift, aging, and temperature dependence are also less sensitive [7]. In fact, analog systems in industry are increasingly being replaced with digital ones [6].
- ***Switchable manual and autonomous input signal control.*** At times, in particular when debugging issues, it is advantageous to have manual control over the input signal set-point. However, as it is desired to generate temperature profile waveforms, manual control would be impractical. As such the system should be capable of easily switching between a manual and autonomous mode.
- ***PIC microcontroller unit (MCU) based autonomous input signal generation.*** For the same reasons why a digital controller is desired, the signal generation system should also be digitally operated. An adjustable analog system to generate various waveforms would be difficult to design and more so to modify. Programmability makes the signal generation a simple matter of scripting a few lines of code.
- ***Synchronous operation with external signals.*** In the same way the system should be capable of operating in a manual or autonomous set-point mode, the system should be capable of accepting an external signal as input. In addition, it is desired to feature a synchronized output mode with external clock signals. This is implemented with the autonomous signal generation system. Timed output is advantageous for associated systems requiring correlation between measurements and system temperature (e.g. DBF laser wavelength tuning).

- *Set-point signal protection.* In the event that an input method should fail or an unacceptable set-point value is received, a protection circuit must reset the set-point to an acceptable value. This is to prevent the current controller from ever driving the TEC module with an inappropriate current. If the input should return to a tolerated value, the protection circuit should automatically switch control back to the input.

## **3.2 Component Selection**

After identifying the requirements, the next step in the design of the electrical system is to select which components to use. The number of potential choices for each component seems endless, with several different manufacturers advertising different advantages. An exhaustive experiment would be too time-consuming, so the main considerations for component selection are price and availability. The main components to consider are the programmable microcontrollers, current driver, and TEC module. Other elements require less scrutiny for selection

### ***3.2.1 PIC Microcontroller Units***

The microcontrollers selected for the system are primarily selected based on availability; however ease of use, cost, and available packaging are also considered. The lab has several PIC units available. PICs are a specific family of microcontrollers made by Microchip Technology, and the units in use are the PIC18F4431 chips. The first algorithms for waveform generation, external synchronization, and PID control were programmed on these chips. They have since remained in the presently designed system.

While there are several microcontrollers on the market, PIC microcontrollers remain a popular selection in digital control for several reasons. During the course of this project, one of those reasons has been their extensive documentation. The PIC18F4431 chip features several analog-to-digital converter (ADC) channels with 10-bit resolution, and a synchronous serial port module. It also features a core clock up operation up to 40MHz and priority levels for interrupts. Reprogramming of the chip's flash memory is performed with Microchip Technology's PICKit3 In-Circuit Debugger/Programmer on the MPLAB Integrated Development Environment.



While the PIC18F4431 chips have been extensively used, after having experienced the system operation in full, consolidation of features is possible. Considerations have already been made to select a PIC microcontroller with the minimal feature requirements covered. In waveform generation including external synchronization capabilities, two external interrupt sources, a serial port, an external timer with interrupt handling, and at least one digital input/output port are the minimum feature requirements. For basic PID control only two ADC channels and a serial port are required. The serial port for both options is necessary for interfacing with separate digital-to-analog converters (DAC). Finally, the core clock of the chip is also an important consideration. Select the fastest core frequency for the fastest calculations and response.

### 3.2.2 Peltier Current Drivers

The primary selection base for the Peltier drivers is cost as several manufacturers offer switched mode based thermoelectric cooler controllers. With the possible exception of the TEC module itself, the most expensive element of the electrical design will be this driver chip. Prices often range between twenty to forty dollars. Most advertise similar features leaving selection up to application specifics. For this project in addition to the bidirectional current requirement, temperature stability is prioritized. Table 3.1 lists three candidate controller chips that were evaluated at the start of this project and several of their features for consideration.

**Table 3.1. Candidate Peltier Driver Controllers.**

| <b>Device</b> | <b>Voltage Supply</b> | <b>Current Supply</b> | <b>Operating Temperature</b> | <b>Setpoint Stability</b> | <b>Price</b> |
|---------------|-----------------------|-----------------------|------------------------------|---------------------------|--------------|
| DRV591        | 2.8V-5.5V             | ±3A                   | -40°C-85°C                   | N/A                       | \$23.94      |
| LTC1923       | 2.7V-5.5V             | ±N/A                  | -40°C-85°C                   | 0.1°C-0.01°C              | \$31.60      |
| MAX1968       | 3.0V-5.5V             | ±3A                   | -40°C-85°C                   | 0.001°C                   | \$22.41      |

The present controller used in the system is MAX1978 by Maxim Integrated, a sister product of the MAX1968 controller listed above. Its selection is based on its advertised temperature stability of 0.001°C. MAX1978 offers the same features as MAX1968 and adds built-in integrator and instrumentation amplifiers. These features are ultimately not used in the present system due to performance issues and difficulties in modifying their designed implementation.

### ***3.2.3 TEC Modules***

After having selected the programmable units and the TEC controller, the next object for consideration is the TEC module. Deciding on the appropriate device can require several steps before selection. First, a weeding process of TEC options not compatible with the designed electrical requirements (e.g. maximum driving current below 3A) is required. After the available units have been identified, proceed next with sorting the physical properties of the TEC required for the particular application the system will be used for. For example, perhaps this system is meant to be applied in a DFB laser tuning environment. Modules with small form factors on the order of several millimeters should be focused on, since DFB lasers are quite small. Once all other requirements are met, dimensions and otherwise, the final step is to consider the cooling capabilities and operable temperature ranges of the remaining TEC options.

As was briefly touched upon earlier, there are two major considerations to be made in the final selection of the TEC unit. The first consideration is for the desired operating frequency of the system. Cooling capacity defines the amount of energy transported per unit time. For a quick TEC response, maximizing the cooling capacity is appropriate. However, in prioritizing for heat transport, a limit is set on the operable temperature range for the device. This is the second consideration for selection. As the temperature difference between the hot and cold side of the TEC increases, the cooling capacity of the module drops. When the temperature differential reaches the maximum for a given TEC current the cooling capacity is zero. This indicates that the temperature of the TEC's cold side will be fixed with respects to the hot side temperature.

To demonstrate this relationship, after fabricating the TEC controller circuit two modules available in the lab were tested and their gain response formulated. Figure 3.1 illustrates the plotted results. Gain signals the magnitude of the temperature response. Larger gains mean larger temperature differences. The module with the larger maximum cooling capacity (blue) produces larger gains for higher frequencies. However, its low frequency gain is less than the other module. Effectively, the system's bandwidth is widened for larger cooling capacity modules, and the overall unity gain is dropped.

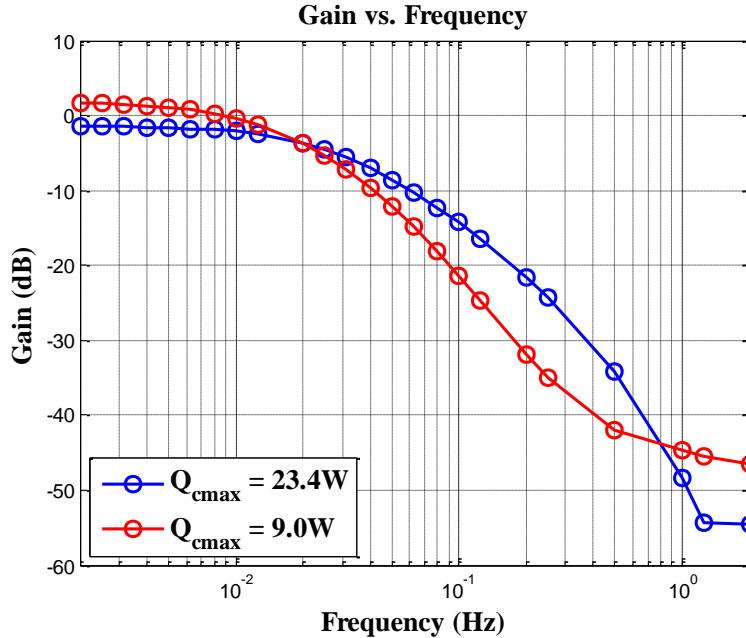


Figure 3.1. Gain response of two TEC modules with different maximum cooling capacities.

The selected TEC module in the final system is the 23.4W maximum cooling capacity module. It is manufactured by Custom Thermoelectric and has part number 06311-5L31-05CFL. The results shown in Chapter 6 are derived with this TEC.

### 3.3 Circuit Design

The last step in the electrical system design is the actual circuit implementation. Appendix C provides the schematic documents representing the present circuit design of the project. The Peltier driver circuit is found in the first sheet, with the microcontroller, and the protection circuit following.

Set-point protection was implemented as two comparators with hysteresis. Each comparator checks the input signal against an adjustable upper or lower bound continuously. When the digital response of either the comparators gets triggered, an analog switch changes the input signal from the present input method to a fixed set-point signal. The fixed signal should be a value where the temperature response is an acceptable state for the particular application or device.

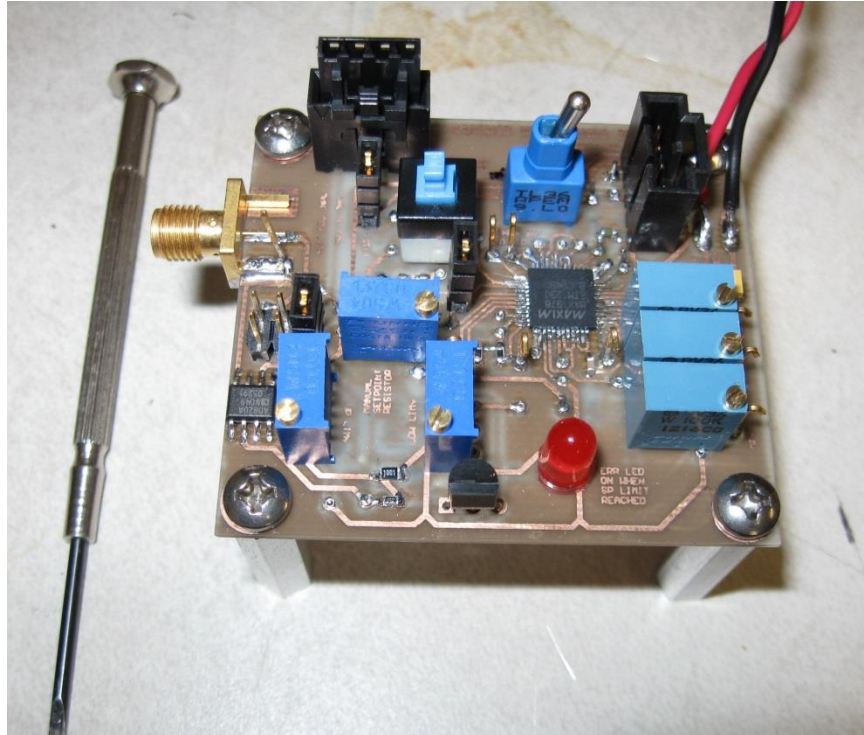


**Figure 3.2. Custom fabricated TEC controller circuit.**

The TEC driver and protection circuit were originally designed and fabricated together. Figure 3.2 depicts the manufactured circuit board without connections and a mini-screwdriver for size reference. The board dimensions are only 2.0"x2.2". The black rectangular features are where the microcontroller and TEC connections are made.

## **Chapter 4**

# **Control System Design and Implementation**

Chapter 3 outlines the electrical system requirements and realizes the control system for the TEC and the test environment is comprised of two parts. In addition, to the digital implementation of PID control, introduced in Chapter 2, the PIC based input signal generator for autonomous set-point control is also considered part of the controller. As the governing dynamics of PID control have already been described, this chapter will briefly discuss only the tuning approach for the system. The main focus of this chapter will address the design for a set-point signal generator that creates temperature specific profiles.

### **4.1 Error Correction Implementation**

The literature review in Chapter 2 provided a thorough background into PID control systems. However, practical design will always be dependent on the particular application and intended use of the controller. In this context mentioning the implementation decisions for the error controller is worthwhile.

Control tasks typically come in two forms: set-point tracking and load disturbance rejection [13]. For either task, every action may not be necessary to implement [4] [5] [6]. In set-point tracking the objective is obvious; follow the reference signal and adjust the plant until the error is tolerable. Load disturbance rejection concerns errors where the plant experiences a loaded response and the controller must force the plant back to reference. A simple example would be cruise control on a car. The controller attempts to maintain a single speed, but an uphill climb slows down the car. To maintain the reference speed, the controller must increase the gas [13]. In this project it has been assumed load disturbances will be rare for most applications. The primary task is thus optimal set-point tracking.

As been described in the system requirements, input signal generation is expected to produce specific temperature response waveforms. However, simply predicting and designing a controller to suit these waveforms cannot be modeled and developed easily. The TEC thermal behavior is

inherently nonlinear and dynamic, and parameters of the controller will often vary in optimal values under different operating conditions [12]. Fortunately, the TEC's temperature response is slow occurring over several seconds. This allows controller tuning to occur in real time and by simple changes to the PID algorithm.

Since the input signal of the system has several potential forms (e.g. fixed set-point, triangle wave, sinusoid), the choice input signal to tune against was the step response. Tuning against the step response reflects the most dynamic change possible in the input signal. Calibrating the controller for the shortest settling time against the worst case input signal should generate the fastest set-point tracking response for any input.

When first testing the PID control system, each of the major controller types: P, PI, PD, and PID [5] were explored. Proportional action only controllers generate large oscillations when tuned for a quick response. PI controllers produced greater stability as expected, however settling times were lengthy on the order of several tens of seconds. PD type controllers were found to have poor steady state response, with more significant offset errors than other types. Despite the potential issues with derivative control, the full three term implementation showed the best response. A look at the performance of the PID controller is shared in Chapter 6.

Design and implementation of this digital controller are significant not only for this project, but for any control application. Realization of PID control on a microcontroller permits use in any subsystem in the lab requiring error correction. The present implementation is cheap, simple, and easily reproducible. This design and the acquired tuning guidelines should prove useful in other areas of research.

## **4.2 Temperature Profile Generation**

As previously mentioned, a digitally implemented input signal generator is desired in the set-point control of the TEC controller. The purpose of the generator is not to mimic a typical voltage waveform generator, but to create specific profiles in the temperature response of the TEC chamber. The contrast between these two options results from the nonlinear relationship

between thermistor resistance and temperature. This section of the thesis will explain this contrast more clearly and discuss how the temperature waveform generator is implemented.

A thermistor is a device that changes resistance with varying temperature. The relationship between the resistance and temperature is often modeled by the first-order Steinhart-Hart equation. This equation is exponential and thus introduces nonlinearity into the control system [7]. Typical waveform generators can create linear time domain voltage signals. However, applying these signals to the TEC controller will never invoke a linear time domain temperature response. The implied purpose of a temperature waveform generator is to pre-compensate the nonlinear relationship to generate linear time domain temperature profiles.

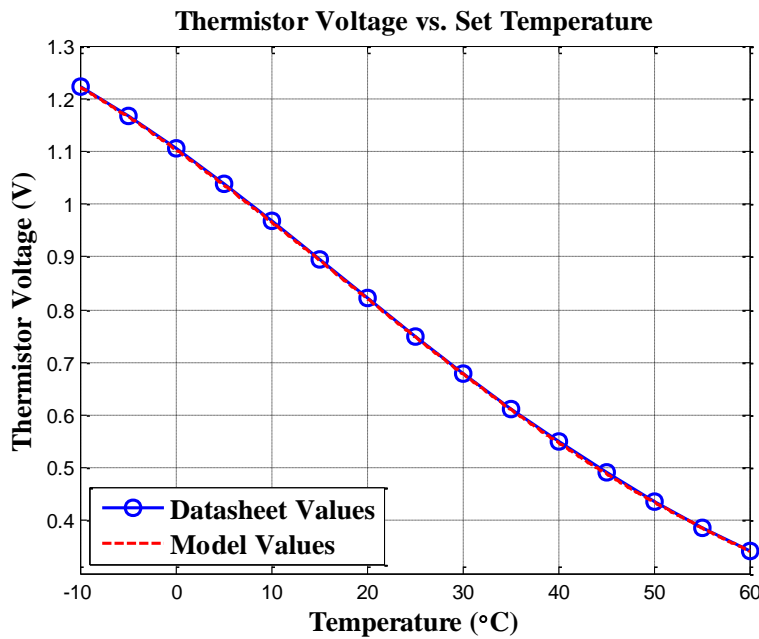


**Figure 4.1. Thermistor voltage model for temperature waveform generator.**

Performing this operation requires a model to relate temperature to the equivalent thermistor voltage. Fortunately, thermistor datasheets often provide a table tabulating temperature against thermistor resistance. Knowing the electrical design of the system, converting thermistor resistance to voltage should be a simple task. The thermistor used in the final product assembly is B57540G0103F000 by EPCOS. Utilizing its datasheet and the electrical configuration of the thermistor, the relationship between temperature and voltage was formulated. Figure 4.1 illustrates the relationship derived from the datasheet and the fitted model used for signal

generation. The configuration of the thermistor can be found in the schematics of Appendix C. With a model equation relating temperature to voltage the only task left in completing the temperature waveform generator is creating the desired temperature profiles. For each waveform, individual functions can easily be scripted to generate this response. A few simplified pseudo-code examples are presented below:

```
// Output Sawtooth Waveform
while(SawtoothOutput == 1){
    for i = 1 to NumberOfOutputs
        CurrentTemp = TemperatureStart + i*TempIncrement;
        SetPointVoltage = TempToVoltCalculator(CurrentTemp);
        OutputVoltage(SetPointVoltage);
    end
}

// Output Triangle Waveform
while(TriangleOutput == 1){
    for i = 1 to NumberOfOutputs
        if (RisingEdge == 1) {
            CurrentTemp = TemperatureStart + i*TempIncrement;
        }
        else {
            CurrentTemp = TemperatureStop - i*TempIncrement;
        }
        SetPointVoltage = TempToVoltCalculator(CurrentTemp);
        OutputVoltage(SetPointVoltage);
    end
    if (CurrentTemp == TemperatureStop) {
        RisingEdge = 0;
    }
    if (CurrentTemp == TemperatureStart) {
        RisingEdge = 1;
    }
}
}
```

In the applied control design, a dedicated temperature conversion function was implemented as well as a triangle waveform generator. The conversion used is a fifth order polynomial equation and is the same model illustrated in Figure 4.1. With a 40MHz core clock microcontroller, full conversion calculations and output cycles respond on the order of 2kHz, stably. The performance of the signal generator thus far exceeds the capable response of the TEC as computed in Figure 3.1. This assures that the output process signal of the system is purely a result of the TEC and PID controller performance. The 2kHz output rate of the signal generator should also permit the formation of high resolution temperature profiles.



### 4.3 External Synchronization

Developing a mode for external synchronization requires an understanding of the synchronizing signals input into the system. The designed synchronizer caters to two clock signals representing the output sampling rate and a directional clock for the output waveform (e.g. high clock signal means triangle output wave should be on the falling edge). Several schemes were tested with a final implementation using the microcontroller's external interrupts, digital input/output ports, and timer features.

Applying the clock signals onto the microcontroller's interrupt channels triggers a priority interrupt service whenever an edge of the clock signal is received. This allows precision timing with the clock signal as the interrupt service halts normal operation until the service routine is complete. Triggering outputs to the DAC off the sampling clock synchronizes the temperature set-point values with the sampling rate. Figure 4.2 shows the external synchronization feature in action.

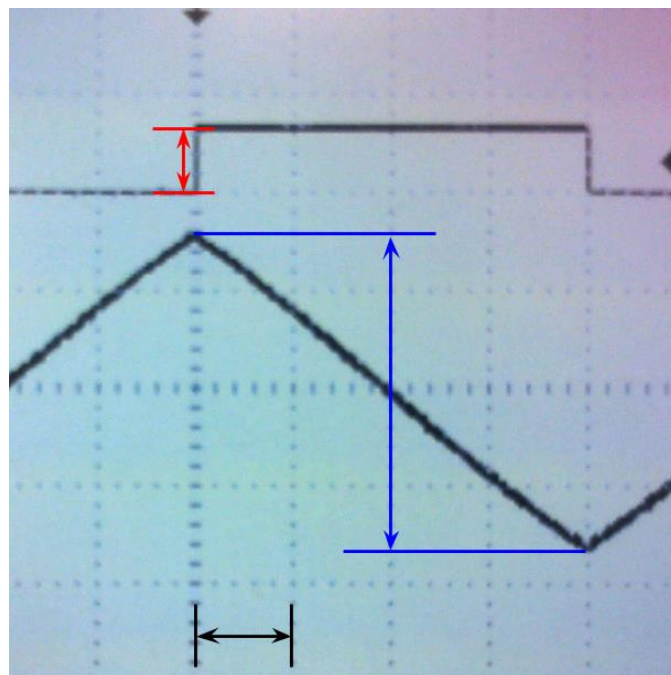


Figure 4.2. Oscilloscope reading of external synchronization in action.

For the setup depicted the direction clock is a 25Hz square wave clock signal and the output response is the falling edge for a high direction signal. The sampling clock, not shown, is a 10kHz square wave signal. The red arrow indicates the amplitude of the direction clock, ~3.5V. Blue arrow represents the output response of a triangle wave from the input signal generator, ~640mV. The black arrow marks a time division spacing of 5ms.

# Chapter 5

## Environment Chamber Design Assembly

After the electrical system and control system design, fabrication of an appropriate TEC housing is required to complete the system assembly. This chapter focuses on the design and fabrication of the environment chamber used in the final product.

### 5.1 Thermoelectric Heat Rejection

In order to create an appropriate heat sink and test chamber for the TEC module, it is necessary to compute the total heat dissipation by the TEC itself. Heat rejection is not a feature of interest for manufacturers. Thus TEC datasheets often provide little if any information on the total thermal energy generated. However, calculating the heat rejected by the TEC is possible with the equations provided in Chapter 2. This section will show how these equations were used to obtain the potential thermal energy generation of the TEC.

#### 5.1.1 Parameter Extraction

At first glance, the equations provided in Chapter 2 require several key parameters be known to calculate the heat generated by a TEC. Parameters such as the *Seebeck coefficient*, the material resistivity, thermal conductivity, and the thermocouple element dimensions are part of the equations. These parameters, however, are likely proprietary and manufacturers will not provide this information freely. Fortunately, every manufacturer is likely to provide several figures in their datasheets relating the TEC's cooling capacity performance to driving current, voltage, and the temperature gradient across the module. From these figures the key parameters may be extracted.

Figure 5.1 presents modeled information generated from the TEC's datasheet. The blue markers indicate approximated points relating cooling capacity to TEC current and the temperature differential. From eq. 2.1, the cooling capacity can be modeled as a second-order polynomial of the input current allowing variables like the resistivity and conductivity to be approximated as

coefficients. Using nonlinear regression a model is estimated by least squares estimation. The red lines indicate the formulated approximations for each case of the TEC's temperature differential.

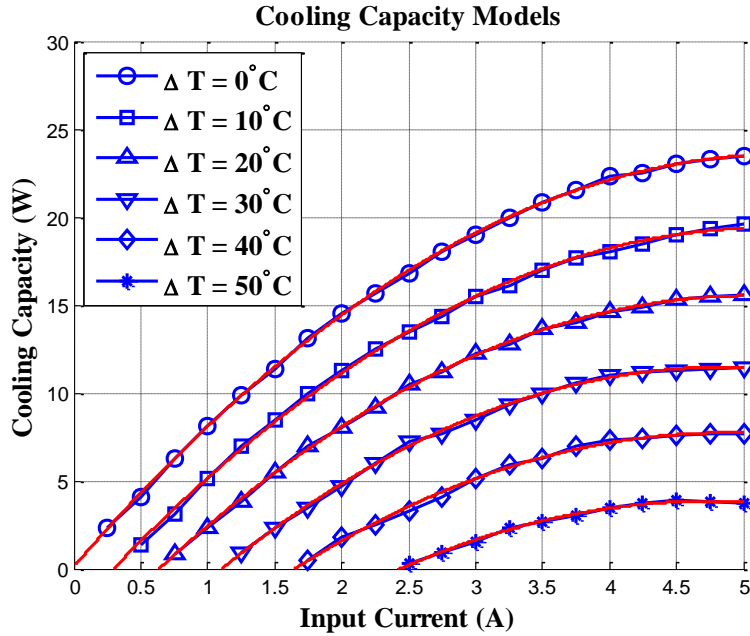


Figure 5.1. Modeled cooling capacity performances for TEC 06311-5L31-05CFL.

### 5.1.2 Waste Heat Formulation

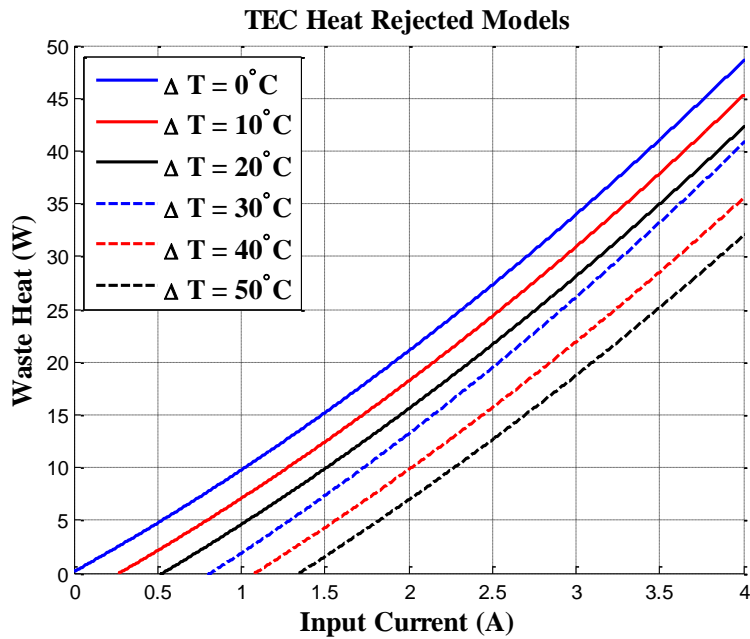


Figure 5.2. Generated waste heat for different TEC temperature gradients.

Using the same coefficients of the models derived, the input electrical power can be calculated by eq. 2.2. The subsequent waste heat generated from the TEC is thus the summation of the cooling capacity and the input power as defined in eq. 2.3. Figure 5.2 illustrates the TEC's heat output as a function of the input current and the temperature gradient. The figure provides the necessary information to evaluate the largest possible heat production by the TEC. Under the system's electrical requirements, the TEC controller will be unable to apply a current greater than 3A. The largest possible waste heat produced by the TEC will thus not exceed 35W.

## **5.2 Heat Sink Optimization**

The primary goal in heat sink design is to formulate a solution with minimal size and cost that will dissipate the thermal energy of the TEC under worst case conditions. Utilizing the equations presented in Chapter 2, this section presents the methodology to formulate a heat sink design solution.

Initially, development of the thermal analysis involved numerical methods to interpolate an optimal solution. However, given the sheer number of variables influencing the total heat transfer this method was abandoned. Instead, using pre-manufactured heat sink samples provided by Alexandria Industries, several variables could be fixed; greatly reducing the complexity of the analysis. The product selected was MN4042 made from aluminum alloy 6063-T5. MN4042 has parallel fin protrusions with specific fin dimensions. The thickness, spacing between, and height of each fin are approximately 2.0mm, 3.5mm, and 14.0mm, respectively. Defining the fin dimensions reduces the analysis to three variable parameters.

The final variables of interest are the heat sink length and width dimensions, and the fluid flow velocity. With 35W of potential thermal energy to dissipate, it was realized the thermal design would require forced convection by a heat sink fan. To calculate the total heat transfer as a function of fluid flow velocity a MATLAB script was created (provided in Appendix B. Using some additional assumptions, the complete solution was realized. The assumptions made were as follows:

The first assumption was if the fan is placed directly above the heat sink, the flow of air generated by the fan would not span wider than the width of the fan itself. Instead, it is assumed the flow of air would be confined between the fins and flow in parallel with the direction of the fins. The second assumption made was that if the heat sink's length was longer than the length of the fan, the fan would always be centered over the midpoint of the heat sink. The last assumption is that the worst case ambient temperature is 50°C and the heat sink should function well enough that the TEC hot side temperature is only 15°C greater than the ambient temperature. Under these conditions it is also assumed that the set-point temperature of the TEC will not fall below 25°C. This implies that the worst case temperature differential of the TEC will be  $\Delta T = 50^\circ\text{C} + 15^\circ\text{C} - 25^\circ\text{C} = 40^\circ\text{C}$ . With these assumptions, several more parameters for the total heat transfer calculation can be defined:

1. The width of the heat sink is defined as the width of the fan (80mm).
2. The characteristic length of the fluid flow path is half the length of the heat sink.
3. The film temperature is 57.5°C (average of  $T_s = T_h$  and  $T_{fl}$ ).

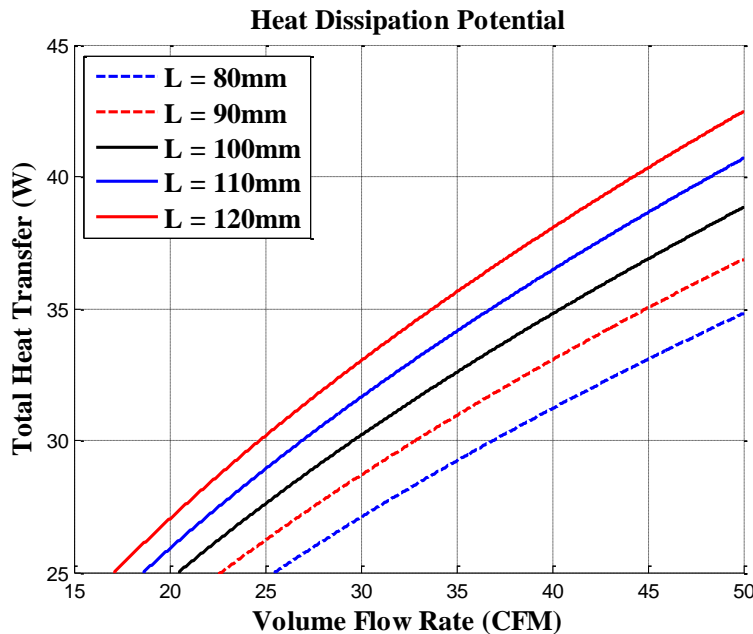


Figure 5.3. Total heat transfer for different heat sink dimensions and fluid flow rates.

The heat transfer profiles for five heat sink lengths were calculated and are illustrated in Figure 5.3. A fan with a volume flow rated at 41.0CFM was found matching the desired 80X80mm fan

dimensions. The minimum length option calculated with a heat dissipation potential greater than 35W at a volume flow rate of 41.0CFM is the 100mm option. Sufficient for the overall design, this solution is the adopted solution for the final assembly. An image of the heat sink and the fan assembly is depicted in Figure 5.4. The system stands in the orientation seen so as not to impede the fan's airflow.



**Figure 5.4. Final heat sink and fan assembly.**

### **5.3 TEC Housing Chamber**

The last topic of discussion regarding the thermal analysis of the system concerns the housing design for the TEC under test. While the environment chamber may seem a trivial matter, there are several caveats worth mentioning. This section briefly describes the major considerations in the housing chamber design.

#### ***5.3.1 Component Swapping***

With adaptability in mind, the housing chamber should permit the exchange of components without damage or compromise in performance. Swappable components include the heat sink and the TEC module. Presently, the heat sink and the chamber are fixed together by screws. If

the TEC module or the application's thermal constraints should change, the screws allow the heat sink to be replaced for a more appropriate design. Embedding the TEC module is a more difficult matter. The sensing surface of the TEC should not physically touch any other object except the sensing thermistor or operating load (e.g. DFB laser, optical sensor). Other contacts would impose an undesired load to the sensing surface and degrade the performance of the system. The present design implements a precision manufactured chamber where the TEC module is wedged and set in place by friction. The entire chamber can be flipped without releasing the module and leaves the sensing surface untouched.

### 5.3.2 Thermally Conducting Walls

The test chamber must also be made from a good thermal conductor for heat transfer to remain efficient. Aluminum is the choice material given its machinability, excellent thermal properties, and structural integrity. However, a point of concern with aluminum is facilitating the electrical connections to the TEC and thermistor while keeping the chamber sealed. The solution implemented uses electrically isolated conductors screwed into the chamber side wall. Figure 5.5 depicts a rendering of the implemented design.

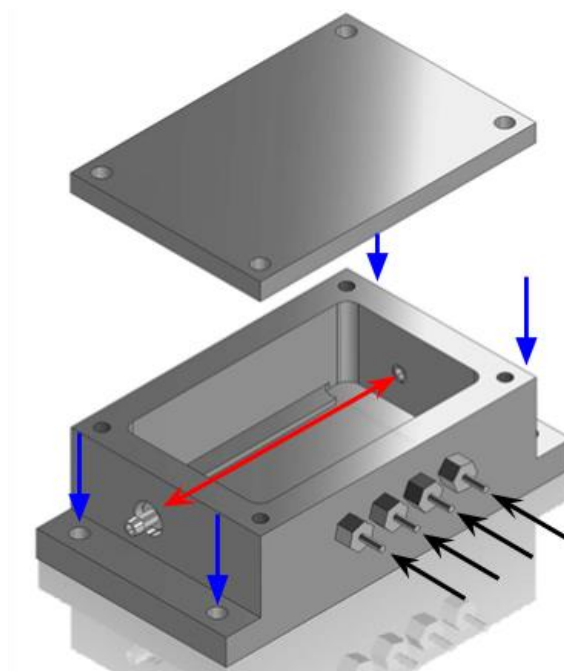


Figure 5.5. Rendering of environment chamber design.



Black arrows point out the mentioned electrical connectors. The central pin of the connectors is electrically isolated from the chamber wall and extends through the screw. Blue arrows mark the screw holes for mounting the chamber against the heat sink, and the red arrow indicates the inlet and outlet ports for optical sensors. The housing is designed to allow the TEC to sit flat on the inside of the chamber floor. Four screws are used to seal the top plate with the rest of the fixture. The cavity above the sensing surface of the TEC serves as the test environment for the system.

### 5.3.3 Thermal Compound

This last discussion regards the use of thermal compound in the designed assembly. It is imperative that some product of thermal grease be used between components. The system will not perform well without it and the reasoning is simple. Regardless of how smooth or flat a surface may appear, microscopically the surface is rough. Thermal compound fills the gap between surfaces with conductive elements and maximizes heat transfer by increasing the actual contact area. Figure 5.6 helps to illustrate this point where arrows represent points of contact.

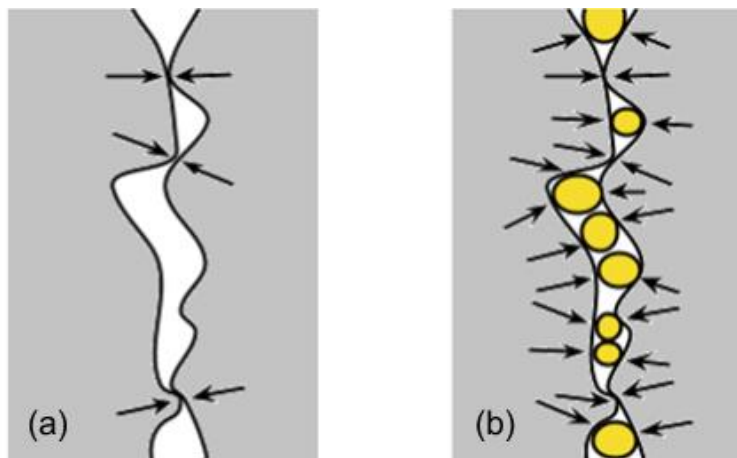


**Figure 5.6. Two surfaces without thermal compound (a), and with thermal compound (b).**

Thermal compound should not, however, be used as a filler material for large gaps. The thermal conductivity of the grease is much greater than air, but is far less than metal. For the thermal design of this project, it is recommended that any changes on the surfaces directly between the TEC module and the heat sink be avoided.

## Chapter 6

# Experimental Analysis of System Performance

With the subsystems designed and fabricated, the next step was to evaluate the performance of the entire system. This chapter discusses the various tests performed and reviews their results. Experiments performed include: tuning the PID controller against a step response, evaluating the system's set-point tracking performance, gauging the system's ambient environment response, and monitoring the system noise.

### 6.1 Experimental Setup

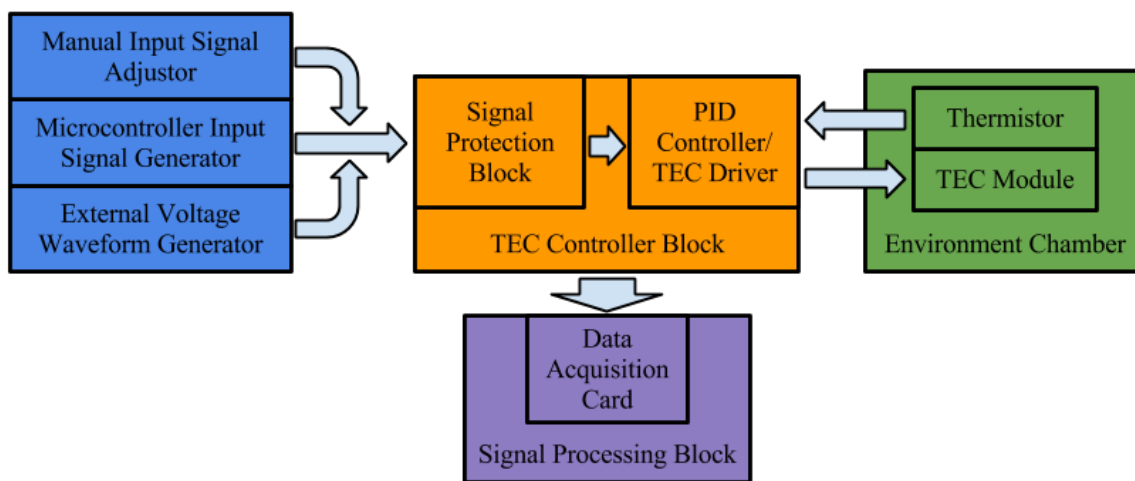


**Figure 6.1. Block diagram of experimental setup.**

Four main blocks comprise the experimental setup. Figure 6.1 illustrates the diagram of the test setup. The first block (blue) contains the various input methods that the system can handle. This includes a potentiometer for manual input signal generation, the microcontroller based signal generator, and an external port for function generator input. This block feeds into the control elements in the system. In the control block (orange), the input signals are checked against adjustable voltage limits and passed along to the PID controller. The passed signal serves as the reference set-point signal. Control signals calculated by the PID controller are fed into the Peltier driver whom generates a proportional TEC current. The TEC module, located in the environment chamber block (green), responds accordingly to the applied current. The temperature signal is measured by the sensing thermistor and returned to the error controller, completing the feedback

loop. Various signals on the control block are probed and monitored with a data acquisition card, specifically National Instruments' USB-6211 multifunction DAQ. In the signal processing block (purple), this sampled data is post-processed in MATLAB.

## 6.2 Step Response Tuning

The first test performed consisted of calibrating the PID controller. Tuning rules and objectives have already been discussed in previous chapters of the thesis, so this section will focus on the results of the tuning scheme. As previously mentioned, the adjustments were made against a step input response. A long period (200s) square wave signal is applied with amplitude of 0.25V, offset to 0.75V. In the temperature domain this set-point signal represents a 7.73°C to 44.14°C square wave. Figure 6.2 illustrates a raw arbitrary single period of the response taken after more than three hours of data collection. The surrounding temperature during testing was room temperature.

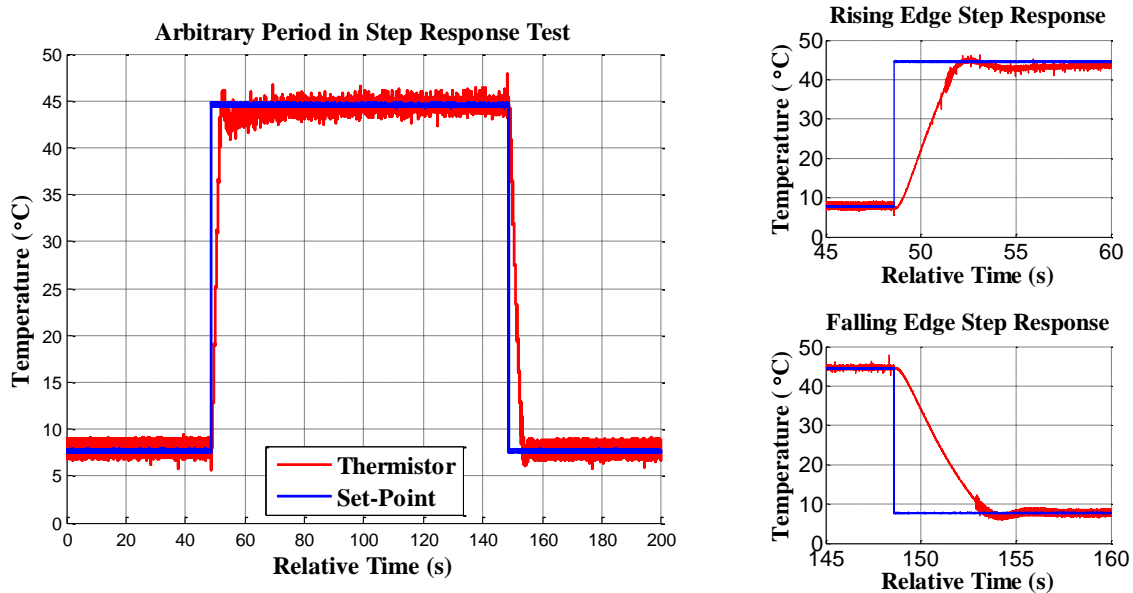
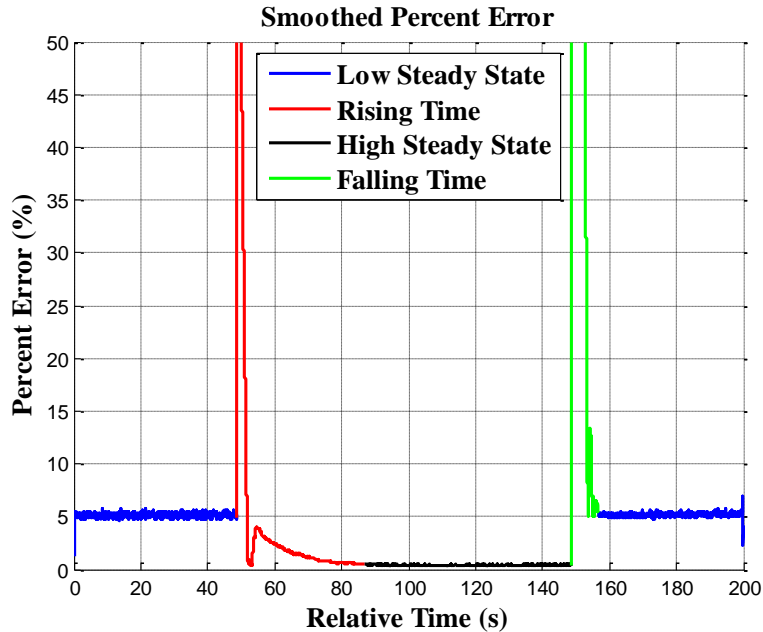


Figure 6.2. Raw signal response to step input signal. Close up of rising and falling edge.

Characteristics of the raw signal response include a  $\pm 0.2^\circ\text{C}$  variation in the set-point signal, a  $\pm 1^\circ\text{C}$  variation in the thermistor signal, a rising edge slew rate of approximately  $13.4^\circ\text{C/s}$ , and a falling edge slew rate of approximately  $-9.29^\circ\text{C/s}$ . It is expected that the TEC would have a faster heating response as Joule heating will always work with thermal generation and against cooling

capacity. However, it is interesting to see that the settling time of the high temperature response is longer than the cool temperature settling time. This can be noted visually and analytically when comparing the time it takes for the percent error response to drop to steady state error conditions after input edge. Figure 6.3 illustrates the percent error response of the data shown in Figure 6.2 after a 0.1s smoothing period.



**Figure 6.3.** Percent error response of data in Figure 6.2.

The sharp points of inflection mark the onset of the step response. The marked flat band regions represent the steady state condition of the system. Interestingly, for the cool period the steady state error is significantly larger than the error for the high temperature region. This illustrates that the PID controller is configured for smaller offset errors at high temperatures, but requires more time to reach steady state. In contrast, low temperature set-points cause the controller to respond with large offset error, but reach steady state quickly.

### 6.3 Set-point Tracking Response

The next experiment performed evaluated the system's ability to accurately perform set-point tracking. The following sub-sections discuss the analyses made for fixed-point tracking and waveform tracking. Experiments were carried out with a room temperature surrounding.

### 6.3.1 Fixed-point Tracking

As stated previously, for fixed set-point applications there are two primary goals. The first is for the environment chamber to serve as a temperature reference for other sensors. The second purpose is to maintain the chamber at operable temperatures while the ambient environment may be unfavorable. Surrounding temperature experiments are addressed in a later section of this chapter. Presently, the focus is on temperature reference applications, where priority lies with long-term temperature stability and minimal drift.

The fixed-point tracking experiment was left running for several hours at a set-point voltage of  $0.5V = 44.14^{\circ}C$ . Figure 6.4 illustrates the raw signal collected and filtered signal for seven hours of collected data. It can be seen that for unprocessed data, the signal variation can be as much as  $\pm 2^{\circ}C$  in both the set-point signal and the thermistor response. After filtering, the variation can be reduced to a  $0.05^{\circ}C$  variation in the set-point, and  $0.1^{\circ}C$  in the thermistor response. A third-order Butterworth low-pass filter with cutoff frequency at 100mHz was used to create the data shown.

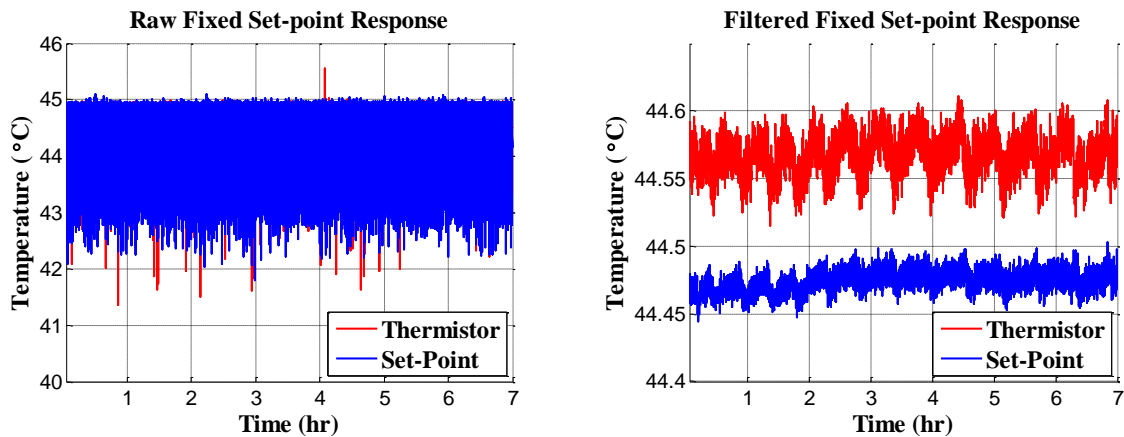


Figure 6.4. Fixed set-point input with raw and filtered response.

Inspecting the percent error of the signal reveals that the raw signal has an average error less than 0.5%. After filtering the average percent error can be improved to about 0.2%. Figure 6.5 also reveals even after seven hours of run time the percent error after filtering never exceeds 0.3%. However, the percent error of the raw signal reveals that at various points in time the response of the thermistor will have as much as 7% error from the expected value. From on this response it would be appropriate to implement an analog filter for the thermistor response. This should help

improve the measured signal quality as well as aid in the PID controller operation; it was previously discussed how signal noise is a detriment to the derivative action of the controller.

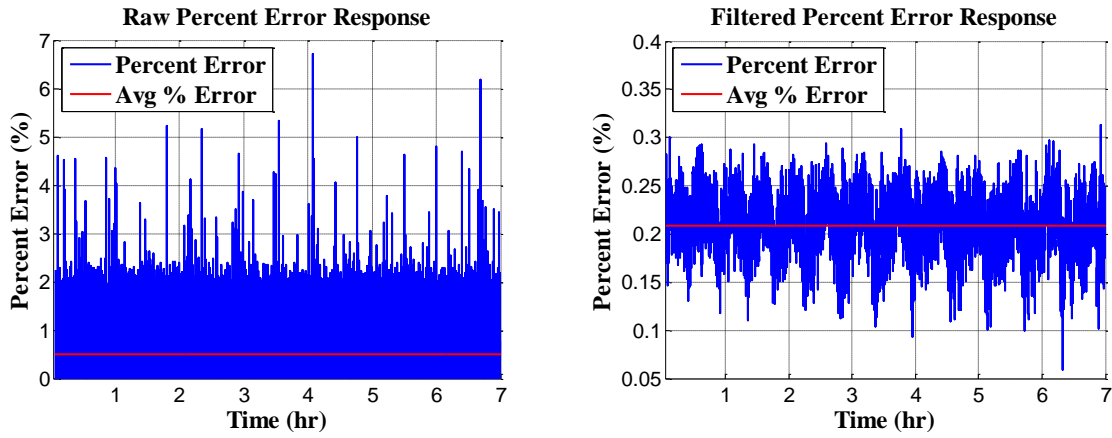


Figure 6.5. Percent error response of the fixed-point tracking experiment.

Performing a linear fit to the filtered percent error reveals a drift of approximately 0.0015% from the expected value over an hour. This shows the system performs with good stability even over long periods of time. It is expected that most optical systems the chamber would be used for would not operate for much longer than a couple hours. However, if longer periods are required, then further testing is required.

### 6.3.2 Waveform Tracking

Waveform tracking experiments were performed similarly to the fixed set-point experiment. Data collection ran for at least three hours with a sinusoid and a triangle waveform tested. The results shown in the Figure 6.6 are for a period of the signal selected at random during the third hour of measurement. Both waveforms have an input period set to 200s with the same amplitude and offset described for the step response signal in Section 6.2.

Characteristics of the sinusoidal response after filtering include a high temperature offset of 0.35°C with a 1.92s time lag and a low temperature offset of 0.45°C with a 2.41s time lag. The triangle waveform response has a high temperature offset of 0.58°C with a 0.73s time lag and a low temperature offset of 0.63°C with a 0.96s time lag. The smaller attenuation and phase lag at the high temperature end of the waveform is expected given the cooling capacity should be

smaller than the heat generation. Since the set-point signal is continuously changing there are no settling time issues with the error controller. The thermistor response appears to retain the shape of the input signal quite well. However, distortion that occurs is greatest at the turning points of the input signal.

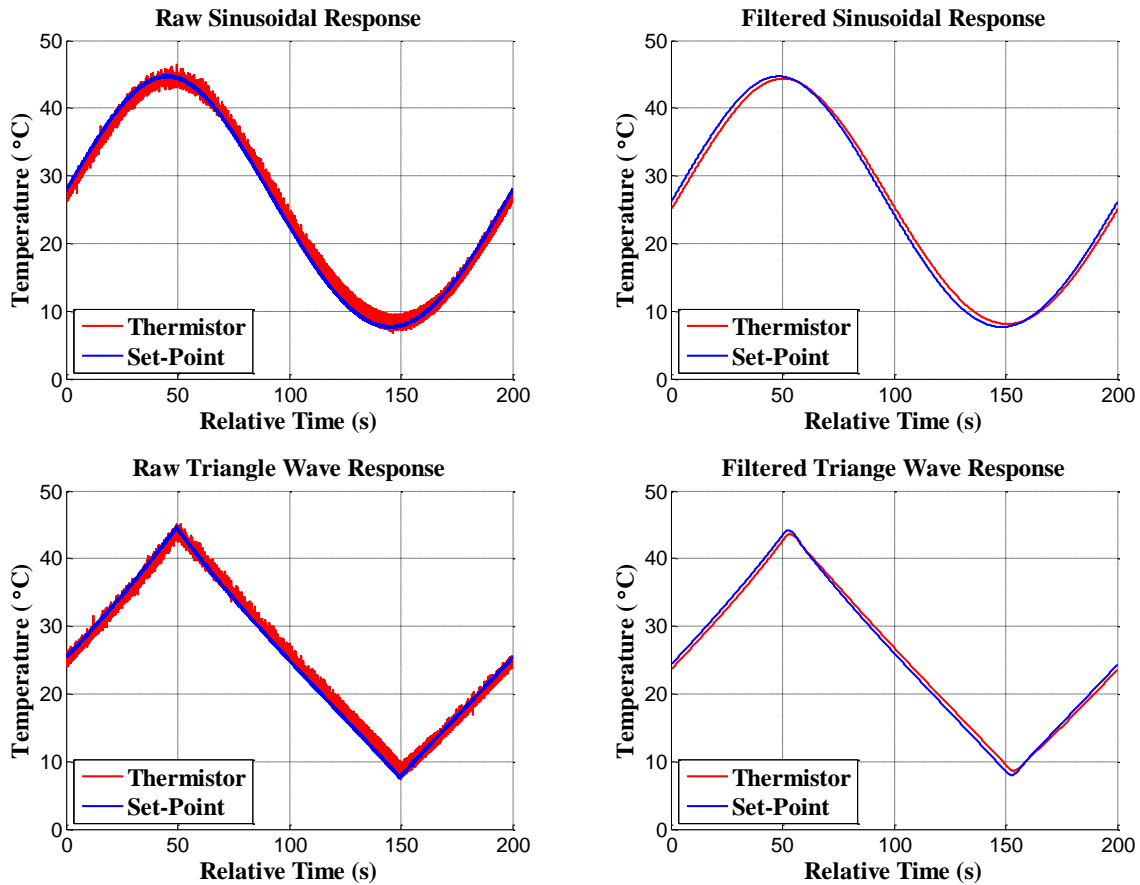


Figure 6.6. Raw and filtered response signals for sinusoidal and triangle wave input.

A standard means to evaluate the set-point tracking responses has not been established, though performance should largely be gauged on the particular application of the temperature controlled environment. For example, the response of the systems holds well to the input signal shape given the long period of the signal. If the period is reduced and the input operates on a much higher frequency the distortion in the system should become more apparent as the TEC will not be able to respond as quickly. However, the amplitude of the input signal covers  $>30^{\circ}\text{C}$  in temperature change. It is believed if the scale of the overall signal, in the amplitude and period, are scaled proportionally the distortion effects should remain the same. This implies the same quality signal

response should be achievable at higher frequencies if the applied system allows for the smaller temperature scanning operation. Again the limits and definitions of the acceptable distortions will depend on the application.

#### 6.4 Ambient Temperature Response

The next tests performed regard the evaluation of the system's ability to tolerate changes to the ambient environment. As previously discussed the environment chamber is thermally designed to handle TEC temperature differentials of 40°C. The design is intended to be sufficient for a room temperature (25°C) set-point in a 50°C ambient environment. This section of the thesis discusses how the system performed against an ambient environment of approximately 50°C and 5°C with a 25°C set-point temperature. Figure 6.7 plots the filtered signal response of the system under each test.

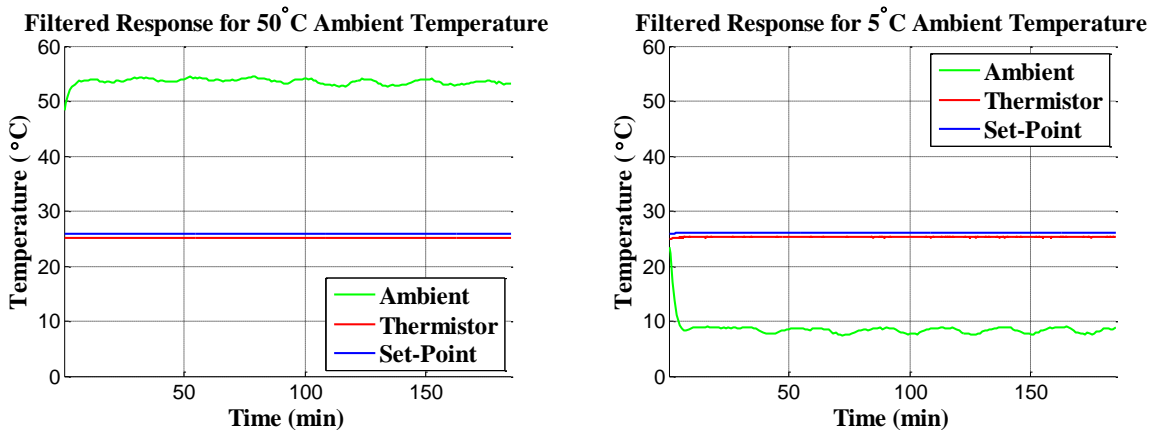


Figure 6.7. Filtered temperature response of system with ambient temperatures of approximately 54°C and 8°C.

The test setup was placed inside a commercial-grade refrigerator/furnace. Data was collected for over three hours while the temperature of the refrigerator/furnace was set to 50°C and 5°C. Ambient temperatures were monitored with a thermocouple sensor placed outside the TEC housing chamber. An offset of one degree between the thermistor and the set-point temperature occurs in both test cases. However, both cases show that temperature of the housing chamber remains constant despite fluctuations in the surroundings.



## 6.5 System Noise

For any electrical system, noise can be expected. During the system evaluation several signals were monitored and tested as potential sources of noise or those strongly affected by noise. Of the data collected there are two noise related signals worth mentioning.

The first of the signals is the electromagnetic interference (EMI) response of the system. As stated previously with switched mode based drivers, EMI can be an issue. There is a strong possibility that the inductors for the driver filter generate enough EMI to affect the overall performance of the system. Figure 6.8 illustrates the differential EMI measurement from a turned wire loop placed roughly 1cm from a driver inductor. The figure also illustrates the EMI signal response from the same physical position with a grounded copper shield placed between the loop and the inductor.

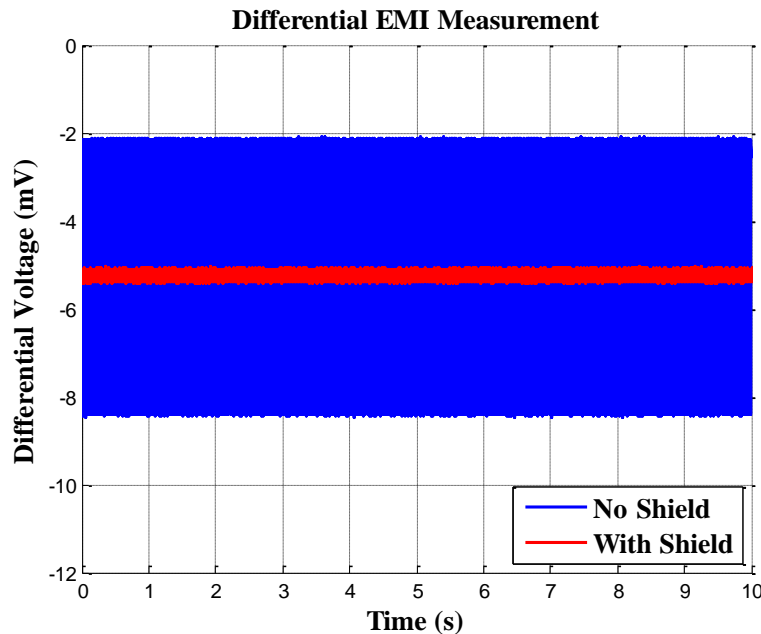


**Figure 6.8. Differential EMI measured at 1cm from an inductor on the controller circuit board.**

The results show there is a significant reduction in EMI signal when the inductors are shielded. Presently without shielding, the inductors are potentially introducing noise into neighboring traces on the circuit board layout. Reconfiguration of the layout would be required to confirm this possibility.

In addition to measuring EMI, the other signal worth mentioning is the voltage reference signal provided by the Peltier driver. The driver's datasheet advertises that the variation in the reference signal at maximum is 5mV. However, this level of stability is not realized in the present implementation of the driver. Figure 6.9 illustrates the variation in the reference voltage signal under a fixed set-point operation.

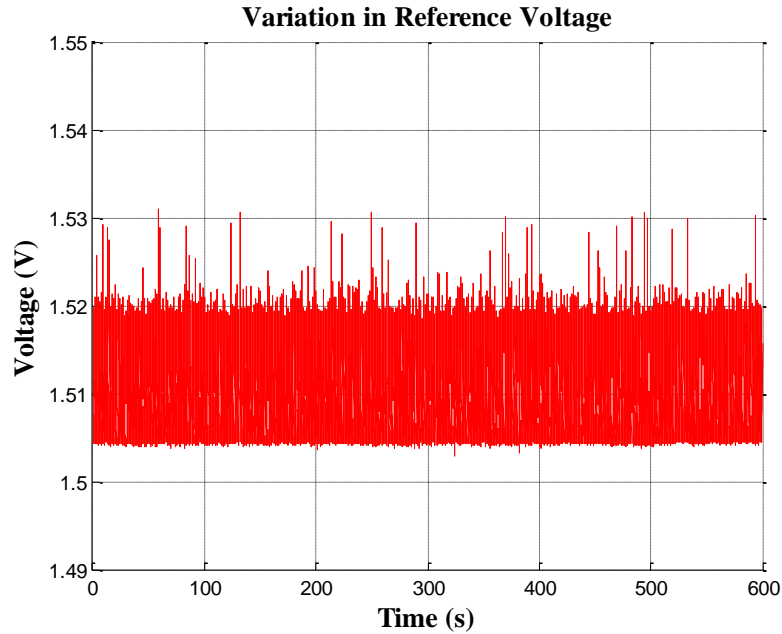


**Figure 6.9. Variation in reference voltage during a fixed set-point operation.**

The variation in the reference signal appears as 16mV, over three times the advertised maximum. Noise in the reference signal has major implications on the performance of the system as it governs the thermistor voltage. A 5mV variation in the thermistor voltage equates approximately to a 0.35°C variation in the temperature domain. Thus the current operation of the system functions with a significant temperature noise measurement. This lowers the temperature resolution the system is capable of even with filtering of the signals. The exact cause for the noise in the reference signal is unknown. It could be a result of the EMI just previously discussed or it could be an issue with the system's power supply. Further investigations are left for future research.

## **Chapter 7**

### **Conclusion and Future Work**

This thesis presents the research and design for a temperature controlled chamber by actuation of a thermoelectric cooler. In this chapter a summary of the completed tasks and a discussion on recommended paths for future study are provided.

#### **7.1 Summary of Work**

A desire for a simplified, cost effective solution in temperature control motivated the creation of this work. This and other motivations impose several overall requirements for the project, which are discussed in detail in Chapter 1. From these general requirements spurred the development of several subsystems with their own individual design specifications. The thesis is made unique by the combined assembly and development of each of these subsystems.

Electrical specifications and desired functionality were part of the first system presented. Utilizing these specifications, necessary elements and components for the project were explored and selected. Decisions were made with strong considerations toward autonomy and compact design. The control system was decided to be implemented with programmable microcontrollers. The minimal microcontroller requirements were provided based on the knowledge gained after testing the system. In other regards, for simplicity reasons and a small electrical footprint the TEC current controller was selected as a commercially available Peltier controller unit. As for the TEC, the design settled on a large cooling capacity, wider bandwidth module. The deciding factor was improving the response time of the system. After the selection of components was realized the electrical circuit was designed and fabricated, with the schematics as previously mentioned provided in Appendix C.

Following the chapter on the electrical system design, implementation of the control system was presented. This included a description of the tuning approach for the PID controller and the digital input signal generator. For the PID controller, the primary performance task was decided as set-point tracking. To best achieve this objective the major concern in tuning the controller

was to ensure a quick yet stable response. The implementation of the PID controller is simple, compact, and easily reproducible. Realization of the digital PID controller itself is a significant development from this project. The chapter also describes the creation of the temperature waveform generator. Formulating the solution involved modeling the temperature to voltage relationship of the thermistor, and using code to generate specific temperature profiles. In addition, the chapter describes the requirements and implementation for external synchronization in the input signal generator. This solution was realized by proper utilization of the micro-controller's interrupt services.

The last design topic was the thermal management of the TEC and housing chamber. All the waste energy generated by the TEC during operation should be dissipated by the chamber design. The most thermal energy the TEC could create under worst case conditions was calculated by extracting required parameters from the TEC's datasheet. After recognizing the total heat transfer by the TEC, an investigation for the minimal heat sink design requirements was made. Optimization of the heat sink was formulated by limiting dependent variables, and finding the cheapest solution from available components. The final implementation contains an 80X100mm heat sink cut from a premade commercial heat sink and an 80X80mm fan with a volume flow rate of 41.0CFM. The thermal design discussion ends with the considerations made for the TEC housing where a rendering of the housing is found in Figure 5.5.

Several interesting developments were discovered during the experimental testing of the system. When calibrating the PID controller against a step response it became clear that the same PID parameters suitable for high temperature set-points may not perform equally for low temperature set-points. High temperature operations have low steady state error but long settling times. Low temperature operations have high steady state error but small settling times. Additionally, it was found with the parameters set during calibration, the heating slew rate of the TEC is found to be  $13.4^{\circ}\text{C/s}$  and the cooling slew rate to be  $-9.29^{\circ}\text{C/s}$ .

During fixed set-point testing it was found that averaged error offsets are less than 0.5% for the raw thermistor signal. After filtering that offset could be reduced to about 0.2%. The calculated temperature drift from seven hours' worth of collected data is less than  $0.0015^{\circ}\text{C/hr}$ . These tests

in conjunction with the waveform tests show that filtering helps significantly in drawing out a cleaner signal from the raw data. Filtering also helps to improve temperature resolution to within  $0.1^{\circ}\text{C}$  in the thermistor response. The waveform tests show the system performs well with set-point tracking and the original signal shape is held with minor distortions in the response.

For ambient temperature analysis the results show the controller is capable of maintaining the set-point value despite temperatures as high as  $54^{\circ}\text{C}$  or as low as  $8^{\circ}\text{C}$  in the surroundings. This performance suggests the system is suitable to perform in most typical lab environments. Finally, a discussion on the signal noise was presented. The  $0.1^{\circ}\text{C}$  temperature resolutions stated previously are only achieved through filtering of the thermistor signal, post data collection. Measurements found a large amount of voltage noise on the reference voltage signal that is used to drive the thermistor voltage. A potential source of this noise was identified to be EMI from the Peltier driver's inductors. Recognizing these sources may help future variations of this work improve the temperature resolution of the system.

## **7.2 Suggestions for Future Work**

The work performed over the course of this thesis provides a good foundation for realizing a temperature controlled chamber actuated by a thermoelectric cooler. Even so, there are several areas for potential improvement if the research should continue. This section of the chapter provides a summary of suggested paths for future research.

Development in the electrical design is a good starting point to improve the system performance. The experimental results show a fair amount of system noise in the measureable signals. A likely source of this noise may be the lab bench voltage generator which is known to have a poor signal quality. Investigation into a dedicated low noise, high-current power source should be a worthy investment for future work. An additional point of improvement could be to redesign the circuit layout with stronger considerations toward EMI protection. The results showed that a significant EMI response can be measured from the inductor components on the circuit board. Shielding these components could potentially reduce their effect on neighboring traces, which include the

reference and thermistor voltages. Reducing the overall system noise would help realize higher temperature response resolutions as advertised by the Peltier driver.

Improvements in the error control system are also worth noting. There is increasing literature on improved PID implementations and control. Adaptive error control is one such area and is of particular interest in applications of set-point tracking. The tuning scheme would likely consist of a real-time signal identifier and make adjustments to parameters according to tuning models obtained analytically or experimental [6]. Indeed the results provided in Chapter 6 suggest that different set-points require different control parameters. In this regard, the system may benefit from having adaptable PID parameters that change depending on the temperature set-point. Equivalently, the system could be adjusted for different TEC modules or changes in system applications. Obtaining these parameters, however, will take some effort and considerably more time to implement.

In regards to the thermal design, there is not much more that can be offered in terms of an analytical approach. Previous work by others has always concluded that experimental iterations in the thermal design realize the most optimal performance characteristics. It is suggested that by iterative methods the maximum performance can recover some ten degrees of improvement back toward the ideal performance [10]. Of course the measure of performance will always depend on the task at hand. However, if time permitting, future endeavors could include an experimental approach to heat sink optimization.

## References

- [1] Y. Zhang and J. Ashe, "Designing a High Performance TEC Controller," Analog Devices, Inc., 2002.
- [2] H. Lee, Thermal Design, Hoboken, NJ: John Wiley & Sons, 2010.
- [3] S. B. Riffat, S. A. Omer and X. Ma, "A novel thermoelectric refrigeration system employing heat pipes and a phase change material: an experimental investigation," *Renewable Energy*, vol. 23, no. 2, pp. 313-323, 2000.
- [4] M. A. Johnson and M. H. Moradi, PID Control: New Identification and Design Methods, London: Springer-Verlag, 2005.
- [5] A. Visioli, Practical PID Control, London: Springer-Verlag, 2006.
- [6] K. H. Ang, G. Chong and Y. Li, "PID Control System Analysis, Design, and Technology," *IEEE Transactions on Control Systems Technology*, vol. 13, no. 4, pp. 559-576, 2005.
- [7] D. M. Alter, "Thermoelectric Cooler Control Using a TMS320F2812 DSP and a DRV592 Power Amplifier," Texas Instruments, Dallas, 2003.
- [8] J. Williams, "A Thermoelectric Cooler Temperature Controller for Fiber Optic Lasers," Linear Technology Corp., Milpitas, 2001.
- [9] N. Seshasayee, "Understanding Thermal Dissipation and Design of a Heatsink," Texas Instruments, Dallas, 2011.
- [10] R. J. Buist and M. J. Nagy, "Thermoelectric Heat Sink Modeling and Optimization," TE Technology, Inc., Traverse City.
- [11] A. D. Kraus and A. Bar-Cohen, Design and Analysis of Heat Sinks, New York: John Wiley & Sons, Inc., 1995.
- [12] B. J. Huan and C. L. Duan, "System dynamic model and temperature control of a thermoelectric cooler," *International Journal of Refrigeration*, vol. 23, no. 3, pp. 197-207, 200.
- [13] V. VanDoren, "Disturbance-Rejection vs. Setpoint-Tracking Controllers," *Control Engineering*, 26 09 2011.

## Appendix A – Example PID Implementation

```
// *****
// MCU & DAC Software Ver6.0
//
// The code provided here is a product of work conducted at the Center for Photonic
// Technology (CPT) and is intended for CPT research use.
//
// The function of this program is to implement a digital proportional, integral,
// derivative (PID) controller for error correction in a TEC controller system.
// Setpoint and actual thermistor voltage values are read with the MCU's analog-to-
// digital converters. PID calculations are performed on the read data and output is
// encoded on the serial peripheral interface (SPI).
//
// Revised & Edited by Scott Zhang
// Last Revision: 04/06/2013
// Contributing Authorship: Alan Overby
//
// *****

// *****
// ***** CONFIGURATION BITS
// *****
// Configuration bits require reevaluation upon pin reassignments. See IDE Help & chip
// datasheet for specific details and guidance

#pragma config OSC = HSPLL
#pragma config WDTCN = OFF
#pragma config MCLRE = OFF
#pragma config LVP = OFF
#pragma config SSPMX = RD1
#pragma config EXCLKMX = RD0

// *****
// ***** INCLUDES
// *****

#include <p18f4431.h>

// *****
// ***** DEFINITIONS
// *****

#define PID_CALC_ENA          PORTBbits.RB4
#define DAC_CTL_SIGN         LATDbits.LATD0
#define epsilon               0.0001
#define dt                    0.01
#define Kp                    12
#define Ki                    0.07
#define Kd                    0.005

// *****
// ***** PROTOTYPES
// *****

void main(void);
void init(void);
void highint(void);
float PIDcalc(float, float);

// *****
// ***** VARIABLES
// *****
```



```

static float Vref = 4.96; // DAC reference voltage, specify in Volts
static unsigned short dacl1; // Bit vector for serial input to DAC 1
int ADCinput; // Bit vector storing ADC conversion
float ADCreference = 0; // Reference voltage for MCU's ADCs
float Vactual = 0; // Actual temperature voltage
float Vsetpoint = 0; // Setpoint temperature voltage
float C_PID_Out = 0; // PID calculation output value
float C_PID_corr = 0; // PID corrected output value
float C_DAC_in = 0; // PID calculation adjusted output for DAC

// *****
// ***** HIGH PRIORITY INTERRUPT VECTOR *****
// *****
// Service vector for jumping to interrupt routine, leave as is

#pragma code highvector=0x0008
void highvector(void){
    _asm goto highint _endasm
}

// *****
// ***** FUNCTION DECLARATIONS *****
// *****

#pragma code

void main(void){

    /* Initialize system */
    init();

    /* Define ADC reference voltage */
    ADCreference = 5;

    /* Trigger continual execution of ADC conversion */
    ADCON0bits.GO = 1;
    while(1){
        ADCON0bits.GO = 1;
    }
}

// -----
// INIT(): Initialization function. Sets up core clock, digital I/O ports, global
// variables, interrupts, and serial port interface.
// -----

void init(void){

    /* Oscillator Setup */
    OSCCON = 0x70; // Core clock set for highest frequency
    OSTUNE = 0x3F; // Run at factory calibrated tuned frequency

    /* Initialize MCU ports */
    TRISA = 0xFF;
    TRISB = 0x07;
    TRISC = 0x38;
    TRISD = 0x04;
    TRISE = 0x00;

    /* Interrupt and Timer Configuration */
    RCONbits.IPEN = 1; // 1 - Enable priority levels on all interrupts
    INTCONbits.GIEL = 0; // 1 - Allow for low priority level interrupts
    INTCONbits.GIEH = 1; // 1 - Interrupts enabled
    PIR1bits.ADIF = 1; // 1 - ADC conversion interrupt enabled

    /* Initialization of ADC control registers */

```

```

    ADCON1 = 0b00010000;
    ADCON2 = 0b00110110;
    ADCON3 = 0b11000000;
    ADCHS  = 0b00000001;
    ANSEL0 = 0b00010010;
    ANSEL1 = 0b00000000;
    ADCON0 = 0b00011001;

    /* Turn SPI interrupts off */
    PIR1bits.SSPIE = 0;
    PIR1bits.SSPIF = 0;
    IPR1bits.SSPIP = 0;

    /* Initialize control signal and data vector for D/A converter */
    DAC_CTL_SIGN = 1;
    dac1 = 0x0000;

    /*Enable SPI and configure mode */
    SSPCON = 0x21;
    SSPSTAT = 0x40;
}

// -----
// PIDCALC(FLOAT SETPOINT, FLOAT ACTUAL_POSITION): PID control function. Function
// takes the actual temperature voltage and setpoint temperature voltage as inputs
// and returns a float representing the control signal.
// -----

float PIDcalc(float setpoint,float actual_position)
{
    static float prev_error = 0;
    static float integral = 0;
    float error;
    float derivative;
    float output;

    error = actual_position - setpoint;

    /* In case of error too small then stop integration */
    if((error > epsilon) || (-1*error > epsilon)){
        integral = integral + error*dt;
    }

    derivative = (error - prev_error)/dt;

    output = Kp*error + Ki*integral + Kd*derivative;

    /* Update error */
    prev_error = error;

    return output;
}

// -----
// HIGHINT(): High priority service routine.
// -----

#pragma interrupt highint

void highint(void){

    /* If interrupt is ADC interrupt, proceed */
    if (PIR1bits.ADIF == 1){
        PIR1bits.ADIF = 0; // Reset ADC interrupt flag
        PIR1bits.ADIE = 0; // Disable ADC interrupt while
processing

```

```

if (PID_CALC_ENA == 1){
    while(ADCON1bits.BFEMT);          // Wait until ADC buffer is ready

    /* Get data vector on ADC buffer onto ADCinput */
    ADCinput = (ADRESL);
    ADCinput = (ADCinput >> 6) + (ADRESH << 2);

    Vsetpoint = (float)ADCinput*(ADCreference)/(1024);

    while(ADCON1bits.BFEMT);

    ADCinput = (ADRESL);
    ADCinput = (ADCinput >> 6) + (ADRESH << 2);

    Vactual = (float)ADCinput*(ADCreference)/(1024);

    C_PID_Out = PIDcalc(Vsetpoint,Vactual);

    /* Control Signal Corrections for TEC Controller */
    C_PID_corr = Vactual + C_PID_Out;
    C_DAC_in = C_PID_corr + 1.5;

    /* Adjust output for DAC limits */
    if (C_DAC_in > Vref) C_DAC_in = Vref;
    if (C_DAC_in < 0) C_DAC_in = 0;

    /* DAC output protocol on SPI */
    dac1 = (C_DAC_in * 819);
    dac1 = (dac1 | 0x3000);

    DAC_CTL_SIGN = 1;
    DAC_CTL_SIGN = 0;

    SSPBUF = (unsigned char) (dac1 >> 8);
    while(!SSPSTATbits.BF);
    SSPBUF = (unsigned char)(dac1 & 0x00FF);
    while(!SSPSTATbits.BF);

    DAC_CTL_SIGN = 1;
}

ADCON0bits.GO = 1;                    // Request another ADC conversion
PIE1bits.ADIE = 1;                   // Enable ADC interrupt process
}
}

```

## Appendix B – Heat Sink Thermal Design Calculator

```
function [qtot, Reymax, Vfrwanted] = hscalculator(W, L, Vfrmax)

% Fin dimensions as measure for mn4042, Alexandria Industries
t = 0.002;           % Fin thickness (m)
Z = 0.0035;         % Fin spacing (m)
b = 0.014;          % Fin height (m)

% Cross flow area (m^2)
Ac = b*W;           % assuming L runs along the direction of the fins

% Temperature definitions
Th = 65 + 273.15;   % 65C
Text = 50 + 273.15; % 50C

% Properties of air @ film temperature, 57.5C
Prair = 0.70947;    % Prandtl number
vair = 1.8683e-5;   % Kinematic viscosity (m^2/s)
Kair = 0.028339;    % Thermal conductivity (W/mK)

% Aluminum properties:
kAl = 209;          % (W/mK)

% Characteristic length for flow, assumed half of sink length
Lc = L/2;           % (m)

% Fin related derivations
nf = W/(Z + t);     % number of fins
Af = 2*(L + t)*b;   % single fin area
At = nf.*(Af + L*Z); % total surface area

% Volume flow rate, variable for analysis
Vfr = linspace(1, Vfrmax, 1e5); % (CFM)
Vfr = Vfr*0.000472; % (m^3/s)

% velocities assuming flow is concentrated in the center and flows outward
U = 0.5*Vfr/Ac;

% Reynolds number
Rey = U*Lc/vair;
Reymax = max(Rey);

% Average heat transfer coefficient
h = Kair/Lc*0.664*Rey.^0.5*Prair^(1/3); % (W/m^2K)

% Single fin efficiency
beta = b*(2*h/kAl/t).^0.5;
etaf = tanh(beta)./(beta);

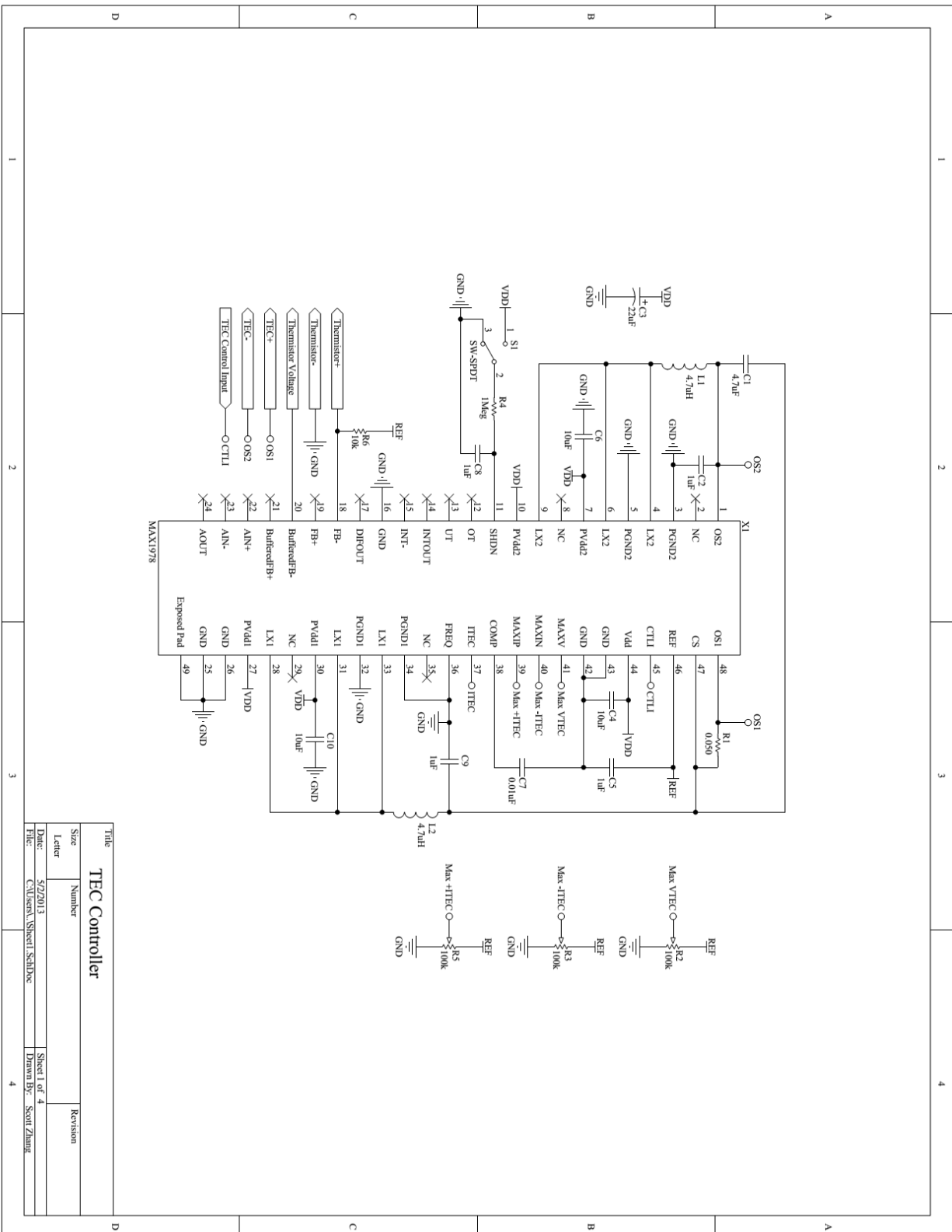
% Overall efficiency
etao = 1 - nf.*Af./At.*(1 - etaf);
```

```
% Total heat transfer
qtot = etao.*At.*h*(Th - Text);

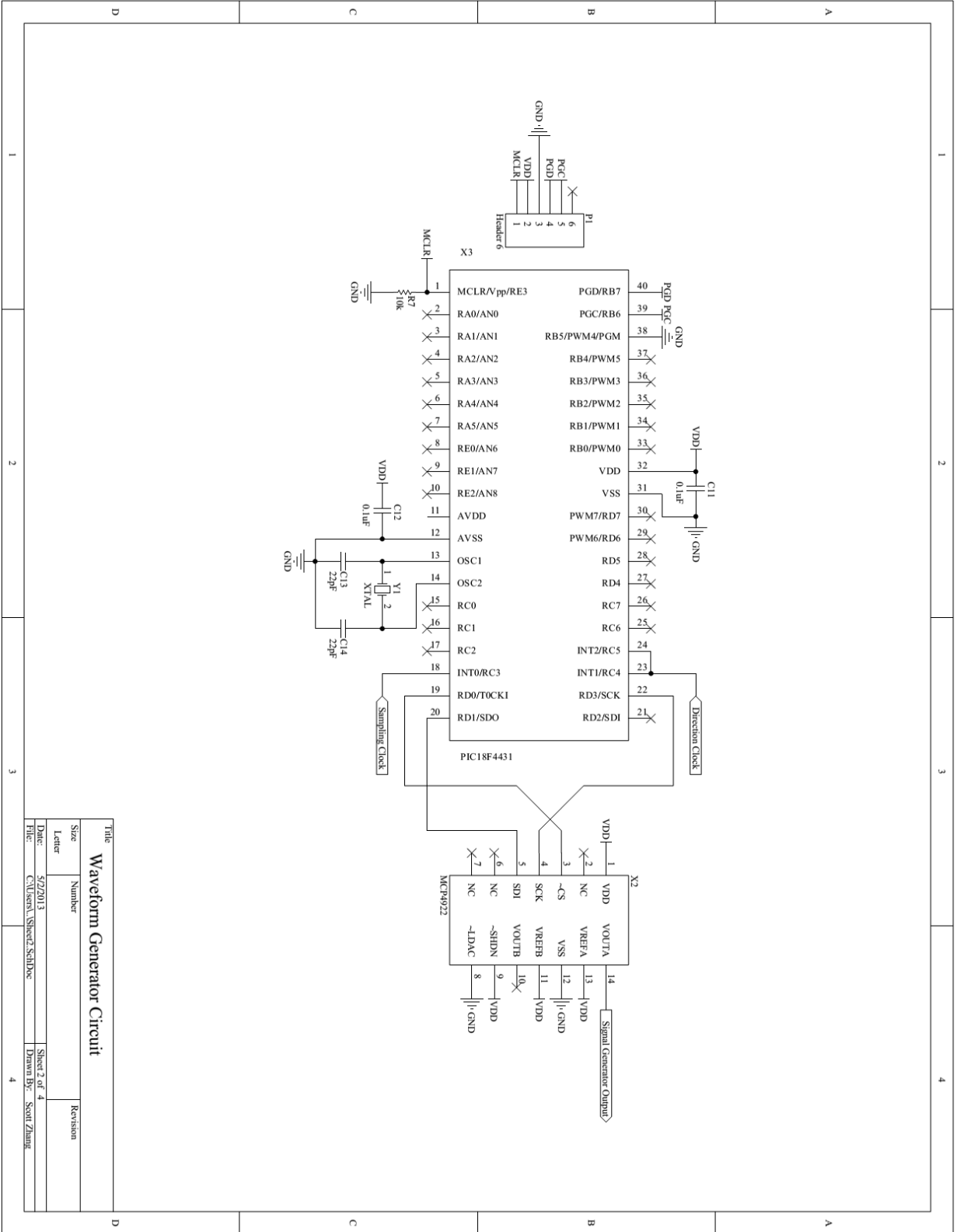
% Necessary volume flow rate for 35W heat dissipation
Vfr = Vfr/0.000472;
Vfrwanted = interp1(qtot,Vfr,35);

end
```

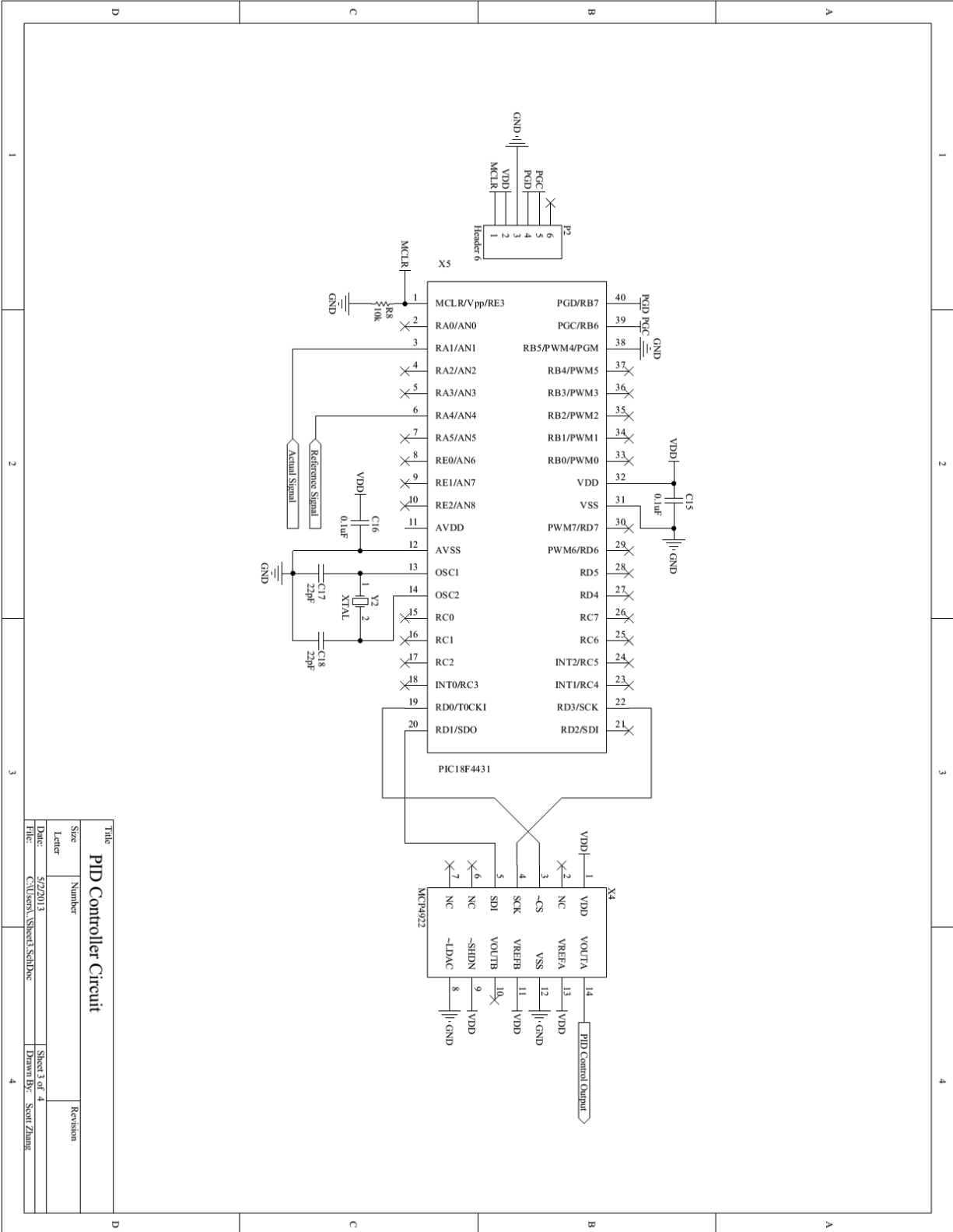
# Appendix C – Electrical Schematics



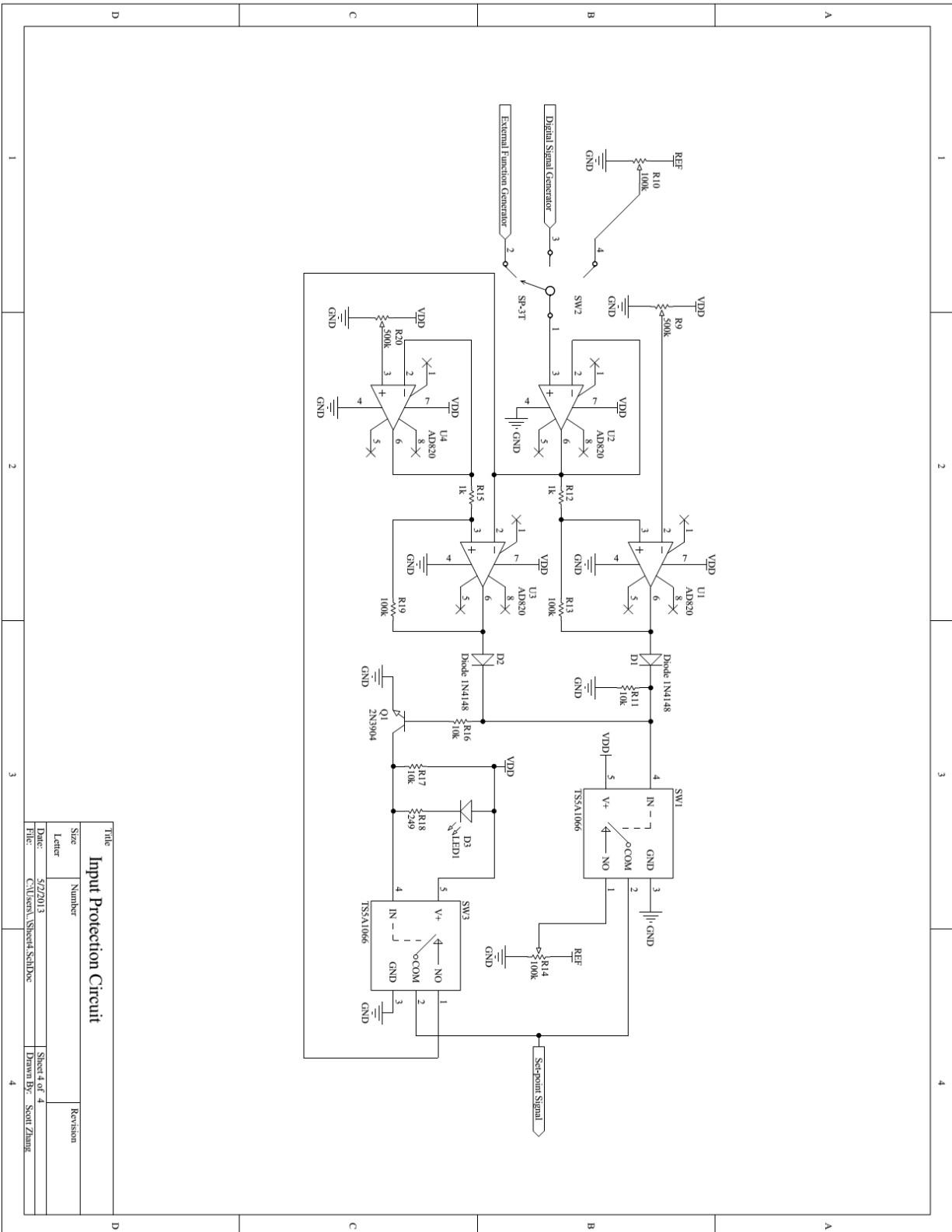
| Title  |                       | Revision              |  |
|--------|-----------------------|-----------------------|--|
| Size   | Number                | Sheet 1 of 4          |  |
| Letter |                       | Drawn By: Scott Zhang |  |
| Date:  | 4/7/2013              |                       |  |
| File:  | C:\Users\Shihai.SNDoc |                       |  |



|                                   |                        |                       |  |
|-----------------------------------|------------------------|-----------------------|--|
| Title                             |                        | Revision              |  |
| <b>Waveform Generator Circuit</b> |                        |                       |  |
| Size                              | Number                 |                       |  |
| Letter                            |                        |                       |  |
| Date:                             | 5/2/2013               | Sheet 3 of 4          |  |
| File:                             | C:\Users\Saint\Desktop | Drawn By: SAINT Zhang |  |







|                          |                         |              |             |
|--------------------------|-------------------------|--------------|-------------|
| Title                    |                         | Revision     |             |
| Input Protection Circuit |                         |              |             |
| Size                     | Number                  | Letter       | Revision    |
| 5722013                  |                         |              |             |
| Date:                    | 5/22/13                 | Sheet 1 of 4 |             |
| File:                    | C:\Users\Wang\Documents | Drawn By:    | Scott Zhang |